



HAL
open science

Fatty-acid based comb copolyesters as Viscosity Index Improvers in Lubricants

Hélène Méheust, Jean-François Le Meins, Annie Brûlet, Olivier Sandre,
Etienne Grau, Henri Cramail

► **To cite this version:**

Hélène Méheust, Jean-François Le Meins, Annie Brûlet, Olivier Sandre, Etienne Grau, et al.. Fatty-acid based comb copolyesters as Viscosity Index Improvers in Lubricants. *European Polymer Journal*, 2022, 181, pp.111674. 10.1016/j.eurpolymj.2022.111674 . hal-03840401

HAL Id: hal-03840401

<https://hal.science/hal-03840401v1>

Submitted on 5 Nov 2022

HAL is a multi-disciplinary open access archive for the deposit and dissemination of scientific research documents, whether they are published or not. The documents may come from teaching and research institutions in France or abroad, or from public or private research centers.

L'archive ouverte pluridisciplinaire **HAL**, est destinée au dépôt et à la diffusion de documents scientifiques de niveau recherche, publiés ou non, émanant des établissements d'enseignement et de recherche français ou étrangers, des laboratoires publics ou privés.



Distributed under a Creative Commons Attribution - NonCommercial - ShareAlike 4.0 International License

Fatty-acid based comb copolyesters as viscosity Index improvers in lubricants

H el ene M eheust^a, Jean-Fran ois Le Meins^a, Annie Br ulet^b, Olivier Sandre^a, Etienne Grau^a, Henri Cramail^{a,*}^a Univ. Bordeaux, CNRS, Bordeaux INP, LCPO, UMR 5629, F-33600, 16, Avenue Pey Berland, 33607, Pessac, France^b CNRS, CEA Saclay, Laboratoire L eon Brillouin, UMR 12, F-91191 Gif-sur-Yvette, France

ARTICLE INFO

Keywords:

Polyricinoleate
Bio-based copolyesters
Lubricant
Viscosity modifiers
Thickeners
Viscosity Index
SANS
Conformational behavior

ABSTRACT

Methyl ricinoleate was functionalized using thiol-ene click chemistry in order to synthesize bio-based comb (co) poly(9-alkyl 12-hydroxystearate)s. The latter were then evaluated as Viscosity Index Improvers in a mineral based lubricant. While most of the poly(9-alkyl 12-hydroxystearate)s investigated behave as thickeners, copolyesters containing 15 to 25 wt% of methyl 9-phenyl ethyl 12-hydroxystearate exhibit a Viscosity Index improver effect, interpreted to a limited solubility of these copolyesters. The effect of these polyesters on the oil viscosity-temperature (V-T) behavior was investigated in the dilute regime of *n*-dodecane used as a model solvent. An aggregation-disaggregation behavior was assumed to explain the V-T behavior observed with these (co)polyesters.

1. Introduction

Lubricants are used in modern engines, industrial machines and equipment in order to ensure a protective film between two metal pieces.[1] Their utilization prevents wear, corrosion and equipment failure. Lubricants are subjected to severe conditions, such as important load and shear and have to ensure a proper lubrication under a wide temperature range. As a result, they are constituted of complex formulations mainly including base oil and several additives to reach the properties required for a given application.[2–5].

One of the major classes of lubricant additives are the viscosity modifiers (VM), representing 25 % of the total additives.[6] Their role is to enhance the oil viscosity at high temperature. Viscosity modifiers are then separate in two categories: thickeners and Viscosity Index improvers (VII). The first ones thicken the oil regardless to the temperature while the second thicken more the oil viscosity at high than at low temperature, as expressed schematically in Fig. 1.

Based on literature, the polymers used as VII can affect the oil viscosity behavior according to temperature (V-T behavior) following two main mechanisms, both based on polymer solubility in oil. The first one, mostly described for comb-like polyalkylmethacrylates (PAMAs), is the coil expansion.[7–10] At low temperature, the polymer coil is isolated in solution with a collapsed conformation, alike in a bad solvent.

[11] By increasing the temperature, the polymer affinity with the solvent increases, thus, the polymer coil expands, counterbalancing the oil viscosity decrease with temperature. The second mechanism is called the aggregation-disaggregation behavior.[12–14] It was observed for copolymers or grafted polymers such as Hydrogenated Styrene Diene copolymers and grafted olefin copolymers-PAMAs (OCP-PAMAs) polymers. Generally, in such a case, the polymers contain an insoluble part and a soluble part against the solvent. The soluble part ensures the polymer solubility while the insoluble part tends to aggregate at low temperature. By increasing temperature, the polymer solubility increases and the coils disaggregate progressively. The polymer effect on the viscosity of the oil is enhanced by the increasing amount of polymer chains swollen by solvent molecules in solution. A schematic illustration of the two mechanisms is displayed on Fig. 1. In both cases, the impact of the polymer on oil V-T behavior is related to its solubility profile as a function of temperature.

Recently, we demonstrated that polyricinoleate and poly(hydroxystearate) polymers show promising properties as VM and more specifically as oil thickener.[15] However, the effect observed remains limited and no VII behavior was observed.

Herein thiol-ene conjugation strategy was used to tune the properties of polyricinoleate (PRic). Methyl ricinoleate was modified by click thiol-ene reaction to introduce dangling linear or branched alkyl chains

* Corresponding author.

E-mail address: cramail@enscbp.fr (H. Cramail).

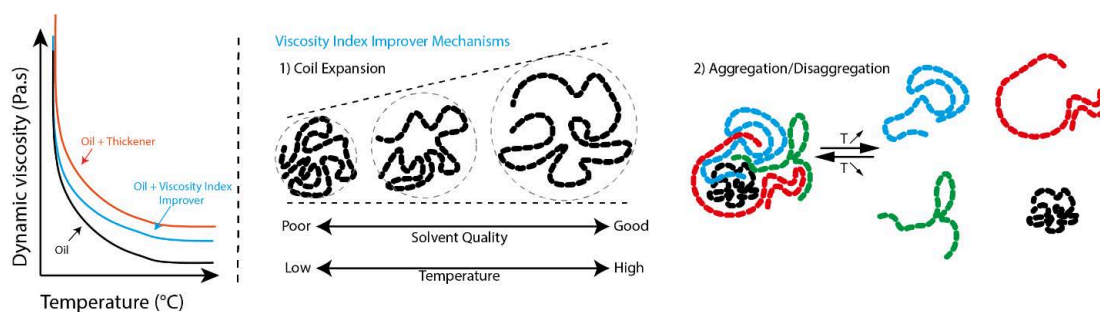


Fig. 1. On the left: Viscosity-temperature relationship of Oil blended with the two types of viscosity modifiers, thickener and VII - On the right: Illustration of two polymeric VII behaviors in solution (1) coil expansion and (2) aggregation / disaggregation[6].

from C4 to C18 as well as aromatic moieties. These new AB monomers were then polymerized leading to comb-like PRic. The impact of the pending alkyl chains on the performances of these polyesters as viscosity modifiers was investigated. In a second part, copolymers were designed based on functionalized methyl ricinoleate backbone bearing insoluble and soluble pendant chains, such as phenyl ethyl and dodecyl moieties, respectively (Fig. 2). Such copolymers demonstrate promising VII properties. Finally, in order to understand how the copolymers behave in solution with temperature and the origin of the VII behavior, their solution behavior was investigated by viscosimetry and small angle neutron scattering (SANS) in *n*-dodecane as a model solvent.

2. Material and methods

2.1. Materials

Bio-based methyl ricinoleate (Nu-chek-prep, >99 %) was used without further purification for functionalization and further polycondensation. Thiols were used as received: butanethiol, octanethiol, 2-ethylhexylthiol, 1-dodecanethiol (>98 %, Sigma-Aldrich), 1-octadecanethiol and 2-phenylethane-1-thiol (98 %, Sigma-Aldrich). 2,2-Dimethoxy-2-phenylacetophenone (DMPA, 99 %, Aldrich) was used as received for photoinitiation. Titanium isopropoxide ($Ti(OiPr)_4$, 99.99 %, Acros Organics) was used as catalyst as received. Reagent grade quality solvents were used as received. Deuterated solvents were purchased from Eurisotop and used as received. Commercial mineral paraffinic oil, the Yubase 4+ (MO) was kindly supplied by TotalEnergies. *N*-dodecane solvent (98 %, Acros Organics) was used as received. Yubase 4+ and *n*-dodecane properties are given in Table 1.

2.2. Comb copolyester syntheses

2.2.1. General procedure of methyl ricinoleate functionalization

All functionalized 12-hydroxystearates were prepared following the same methodology. As a typical example, 10 g of methyl ester ricinoleate (32 mmol, 1 eq.) was mixed with 1-dodecanethiol (19.48 g, 96 mmol, 3 eq.), DMPA was added to the mixture (0.082 g, 0.32 mmol, 0.01 eq.). Photochemical thiol-ene reaction was performed in a 100 mL round bottom flask with a magnetic stirring under UV irradiation. A Lightning cure LC8 fibered light source L9588-06A from Hamamatsu

and a filter A9616-05 (wavelengths: 350 to 400 nm) was used as UV source. During reaction, the conversion of double bonds was monitored by 1H spectroscopy (vinyl proton signals at 5.40 ppm). The irradiation was stopped once the double bond was no more detectable by 1H NMR.

After reaction, the viscous liquid was dissolved in 10 mL of dichloromethane (DCM) and the methyl ester ricinoleate with a phenylethyl/dodecane pendant group was purified by Flash column chromatography, using a gradient of cyclohexane (100 %) to ethyl acetate (100 %) eluent mixture. Flash chromatography was performed on a Grace Reveleris apparatus, employing silica cartridges from Grace. The detection was performed through ELSD and three UV detectors at 254, 265 and 280 nm. Product was recovered with a yield in the range of 62 % – 84 % by solvent evaporation and dried overnight under vacuum (0.22 mBar) at 80 °C and fully analyzed by NMR.

2.2.2. General procedure of polycondensation

The polycondensations were performed following the methodology developed in our previous publication. [15,16].

As an example, the methyl 9-dodecyl 12-hydroxystearate, MRic-C12, (1.5 g, 4.8 mmol) was dried overnight under vacuum at 70 °C with mechanical stirring in 50 mL Schlenk flask at 200 rpm. The mixture was cooled at room temperature under static vacuum and a 5 wt% solution of $Ti(OiPr)_4$ in DCM (0.015 g of catalyst, 0.053 mmol, 1 wt%) was added under nitrogen flow. The mixture was stirred at room temperature for 30 min under static nitrogen then put under vacuum and heated at 70 °C for 30 min. Then the mixture was heated at 120 °C for one hour, 140 °C for another hour and 180 °C for 45 h still under dynamic vacuum to remove the MeOH sub-product and mechanical stirring at 200 rpm. After 48 h reaction, stirring was stopped, the highly viscous mixture was cooled to room temperature and the flask was opened to air in order to stop the reaction.

2.3. Characterization

2.3.1. Nuclear magnetic resonance (NMR)

All the 1H spectra were recorded on Bruker Avance 400 spectrometer at 400 MHz by using $CDCl_3$ as a solvent at room temperature. 1H NMR analyses were performed with 16 scans.

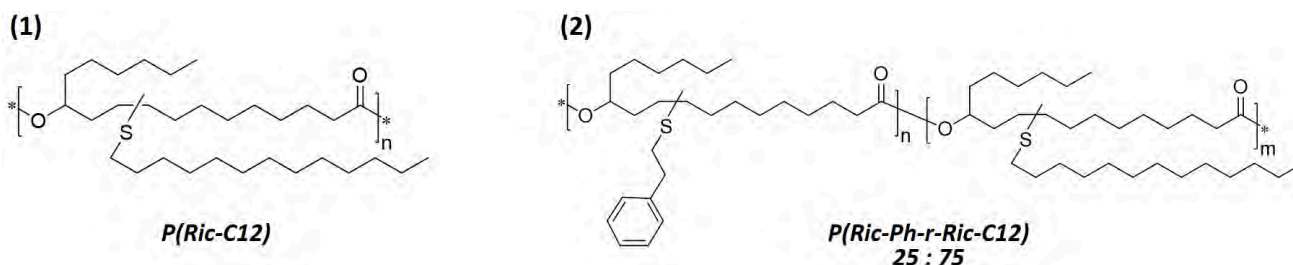


Fig. 2. Chemical structure of homopolymer P(Ric-C12) and copolymer P(Ric-Ph-r-Ric-C12) 25 : 75.

Table 1

Mineral oil and dodecane characteristics, determined experimentally or from producer data sheet [in brackets].

Lubricant oils	Mineral Oil	Dodecane
Density ¹	0.8226 [0.825]	0.749 [0.750]
Mn (g·mol ⁻¹) ²	600	[1 7 0]
D2	1	1
Flash point (°C)	[2 2 0]	[74]
v ₁	18.6	1.005
v at 100 °C (mm ² ·s ⁻¹) ¹	4.3 [4.1]	0.51
Viscosity Index VI	128	–

1- v = kinematic viscosity, 1 mm²·s⁻¹ = 1 cSt; Obtained using a densitometer-viscosimeter at 40 °C.

2- Obtained by SEC in THF, PS calibration, $D = M_w/M_n$, the molar mass dispersity.

2.3.2. Size exclusion chromatography in THF (SEC)

Polymer molecular weights were determined by Size Exclusion Chromatography (SEC) using tetrahydrofuran (THF) as eluent. Measurements in THF were performed on an Ultimate 3000 system from ThermoScientific equipped with a diode array detector (DAD). The system also includes a multi-angle laser light scattering detector MALLS and differential refractive index detector dRI from Wyatt technology. Polymers were separated on three G2000, G3000 and G4000 Tosoh Bioscience HXL gel columns (300 × 7.8 mm) (exclusion limits from 1000 Da to 400 000 Da) at a flowrate of 1 mL·min⁻¹. Columns temperature was held at 40 °C. Polystyrene was used as the calibration standard.

2.3.3. Preparation of oil blended with viscosity modifiers (additives)

Viscosity modifiers were dissolved in the mineral or organic base oils at the concentration of 3 wt%. The mixture was heated at 100 °C overnight under magnetic stirring to promote the solubilization and then cooled down without stirring at room temperature for 24 h. The solubility of the additive in the oil was evaluated macroscopically. Samples were degassed under vacuum and magnetic stirring for 30 min right before being analyzed by viscosimetry.

2.3.4. Viscosity measurements

The viscosimetric tests were performed on a Lovis 2000 densitometer and rolling-ball viscometer apparatus from Anton Paar at several temperatures: 20 °C, 40 °C, 60 °C, 80 °C and 100 °C. Around 3 mL of solutions were added in the densitometer cell and the capillary tube (Ø 1.8 mm for oils and Ø 1.59 mm for dodecane) containing a steel ball (Ø1.5 mm, d = 7.68 g·cm⁻³). The mass density ρ , the dynamic viscosity (mPa·s) and the kinematic viscosity $\nu = \eta/\rho$ (mm²·s⁻¹) are determined directly from the measurements. The relative viscosity was then calculated following equation (1). The kinematic viscosities ν at 40 °C and 100 °C were used to calculate the Viscosity Index (VI) according to ASTM D 2270–10 abacus in order to quantify the VII behavior. [17] The Q values, defined according to equation (2), were calculated from specific viscosities at 40 °C and 100 °C, obtained according to equation (3).

$$\eta_r = \frac{\eta}{\eta_0} \quad (1)$$

$$Q = \frac{\eta_{sp,100^\circ C}}{\eta_{sp,40^\circ C}} \quad (2)$$

$$\text{with } \eta_{sp} = \frac{\eta - \eta_0}{\eta_0} = \eta_r - 1 \quad (3)$$

The relative viscosity (η_r), i.e. the viscosity of mix of additive and oil (η) divided by the viscosity of the pristine oil (η_0), is used to evaluate the contribution of an additive to the viscosity of a solution. It allows then to estimate the thickening efficiency of this additive. The specific viscosity (η_{sp}) is defined as the relative change of oil viscosity brought

by the additive (equation (3)). Then the Q value is defined as the ratio between the specific viscosities at 40 °C ($\eta_{sp,40^\circ C}$) and 100 °C ($\eta_{sp,100^\circ C}$) and, for a given polymer concentration, it is also the ratio of the reduced viscosities (i.e. normalized by concentration) and thus can be interpreted as a “swelling ratio” of the polymer chains in solution. [9,18] Specifically, $0 < Q < 1$ indicates that the thickening power of the additive is less significant at 100 °C than at 40 °C. Conversely, $Q > 1$ indicates the thickening power is more prominent at high temperature in agreement with a true VII behavior. The higher the Q value, the more efficient the additive is to reduce the oil viscosity loss at high temperature.

2.3.5. Dynamic light scattering

Dynamic light scattering measurements were performed at 20 °C with a Malvern Instrument Nano-ZS equipped with a He-Ne laser ($\lambda = 632.8$ nm). Samples were introduced into quartz cells (pathway: 10 mm). The measurements were performed at a scattering angle of 90° at 20 °C.

2.3.6. Small angle Neutrons scattering analyses (SANS)

SANS measurements were performed on the PACE spectrometer of the Laboratoire Léon Brillouin (CEA-Saclay, France). Three configurations were used to cover overlapping wave vector q ranges of $3.2 \times 10^{-3} - 3.4 \times 10^{-2}$, $8.3 \times 10^{-3} - 8.8 \times 10^{-2}$, and $4.4 \times 10^{-2} - 0.45 \text{ \AA}^{-1}$, with the following values of sample-to-detector distance D and neutron wavelength λ : $D = 4.56$ m and $\lambda = 13 \text{ \AA}$, $D = 4.56$ m and $\lambda = 5 \text{ \AA}$, $D = 0.86$ m and $\lambda = 5 \text{ \AA}$. Each sample was measured successively in quartz cells (pathway: 2 mm) at 20 °C, 84 °C, 72 °C, 36 °C and 20 °C back.

By analyzing the scattered intensity curve, it is possible to obtain the characteristic size and shape, and the inter-particle interactions, respectively represented by the form factor $P(q)$ and the structure factor $S(q)$. The classical expression of the scattering intensity per unit volume of spherically symmetric particles is:

$$I(q) = n \Delta\rho^2 V_{\text{part}}^2 P(q) S(q) \quad (4)$$

where n is the number density of particles, $\Delta\rho$ is the difference in the neutron scattering length density between the particles and the solvent, and V_{part} is the unit volume of the particles. The form factor describes the structure of particles and fulfills $P(q=0) = 1$ while the structure factor describes the interaction between particles. In the absence of interactions, $S(q) = 1$. Introducing the volume fraction of particles, $\Phi = n V_{\text{part}}$,

$$I(q) = \Phi \Delta\rho^2 V_{\text{part}} P(q) \quad (5)$$

For individual chains, the volume V_{part} is defined by the weight average molar mass M_w of one mole of chains, the molar mass m and the molecular volume v of one monomer as $V_{\text{chain}} = M_w \cdot v/m$. We introduce the mass density of the polymer (supposedly equal to the one of the monomer) $d = m/(N_A \cdot v)$, where N_A is the Avogadro number ($6.02 \cdot 10^{23}$). For a dilute solution of polymer of weight concentration c , we can express the volume fraction $\Phi = c \cdot d = N_A \cdot v \cdot c/m$, and Eq. (5) then becomes:

$$I(q) = v^2 \Delta\rho^2 \frac{c}{m^2} N_A M_w P(q) = \Delta\rho^2 \frac{c}{d^2 N_A} M_w P(q) \quad (6)$$

Generally, the weight average molecular weight M_w and the radius of gyration R_G can be deduced from the fit to this equation using the so-called Debye function as form factor:

$$P_{\text{Debye}}(q, R_G) = \frac{2}{(q^2 R_G^2)^2} (\exp(-q^2 R_G^2) + q^2 R_G^2 - 1) \quad (7)$$

3. Results and discussion

3.1. Methyl ricinoleate functionalization by thiol-ene addition

Methyl ricinoleate (MRic) was functionalized with several thiols by thiol-ene click reaction in solvent free conditions. The thiols added as second dangling alkyl chain on methyl ricinoleate are illustrated in Fig. 3.

The thiol-ene additions were monitored by ^1H NMR and stopped after complete disappearance of the methyl ricinoleate double bonds. As octadecane-1-thiol is a solid at room temperature, a small amount of cyclohexane was added in the mixture to dissolve it. The other reactions were performed in bulk. In order to ensure a complete conversion, 3 equivalents of thiol were used. The products were purified by Flash Chromatography. Results are summarized in Table 2.

The structures of the purified functionalized methyl ricinoleate were confirmed by ^1H NMR (see SI, Fig S1). The time to reach the complete conversion of the MRic double bond is dependent of the thiol compound added. For instance, the complete conversion was observed within 1.5 h of reaction in the case of butane-1-thiol addition, 3 h with octadecane-1-thiol and 4 h with 2-ethylhexyl-1-thiol. This difference of kinetics may be correlated to the steric hindrance of the thiol compound. The shorter the thiol alkyl chain, the easiest the addition on methyl ricinoleate. In that sense, 2-ethylhexyl-1-thiol is more hindered due to its branched structure, leading to a slower addition on the monomer than butane thiol, for instance. Whatever the thiol nature, the thiol addition occurred mostly on the C10 (at 60 % – 70 %) than on C9 (30 % – 40 %) because of the presence of the hydroxyl function in β of the C9 inducing a slight steric controlled toward C10 position.

3.2. Polymerization of the functionalized monomers

The methyl 9/10-alkylthioether 12-hydroxystearates were polymerized by transesterification. The polyesters obtained are illustrated in Fig. 4.

Two series of poly(9/10-alkylthioether 12-hydroxystearate)s of different molar masses were synthesized. TBD was selected as catalyst for the synthesis of the first series of low molecular weight poly(9/10-alkylthioether 12-hydroxystearate)s. In that case, the reaction mixture was stirred magnetically during 24 h at 140 °C with 5 wt% of TBD. To reach higher molecular weights, the second series was obtained using a mechanical stirring during 48 h at 180 °C and 1 wt% of $\text{Ti}(\text{O}i\text{Pr})_4$. The molar masses obtained for the two series of comb polyesters are reported in Table 3. All the polyester structures were confirmed by ^1H NMR analyses, the spectra are displayed on Fig. 5. The decrease of the methoxy peak at 3.6 ppm as well as the position of the H_β peak in α of the hydroxyl function confirmed the polymerization. The H_β peak is separated in three peaks because the thiol compound can be added on C9 (H_β at 4.9 ppm) as well as on C10. The addition on C10 led to two

different configurations due to the presence of the hydroxyl function in β position of C10 (H_β at 5.05 ppm and 5.1 ppm).

On average, $M_w \approx 10 \text{ kg}\cdot\text{mol}^{-1}$ and $M_w \approx 45 \text{ kg}\cdot\text{mol}^{-1}$ were obtained for the first and second series, respectively. Molar mass dispersity is around 2 for all the polyesters, in agreement with the expect mechanism of polycondensation. Moreover, the M_n values obtained by ^1H NMR using equations established by Carothers are similar to the M_n obtained by SEC measurement, although these were computed from a calibration with polystyrene standards.

3.3. Comb poly(9/10-alkylthioether 12-hydroxystearate) thermal properties

Comb poly(9/10-alkylthioether 12-hydroxystearate)s thermal properties were evaluated in terms of thermal stability and thermo-mechanical behavior for the two series of M_w . The thermal stability was investigated by TGA under non-oxidative conditions at a heating rate of 10 °C \cdot min $^{-1}$. The degradation temperatures defined by a 5 % weight loss ($\text{Td}_{5\text{wt}\%}$) are reported in Table 3. The thermal properties of the polyesters were determined by DSC. The crystallization, melting and glass transition temperatures were recorded from the first cooling and the second heating scans at a rate of 10 °C \cdot min $^{-1}$. DSC thermograms are illustrated on Fig. 6 and thermal characteristic values are reported in Table 3.

The $\text{Td}_{5\text{wt}\%}$ values of the polyesters determined by TGA are in the range 296 – 307 °C. No drastic influence of the side chain nature on the polymer thermal stability was observed. Conversely and as expected, the side chain nature influences the thermo-mechanical properties of the comb polyesters. For instance, PRic derivatives without additional side alkyl chains or with short side chains such as butyl-, phenyl ethyl- or 2-ethylhexyl- pendant chains are fully amorphous. Poly(9/10-alkylthioether 12-hydroxystearate)s with long alkyl side chains, such as dodecyl- and octadecyl- groups, are semi-crystalline with a melting temperature of –37 °C and –5 °C, respectively. The longest the side chain, the highest the polymer melting point and the highest the enthalpy of crystallization, i.e. 46 J/g for P(Ric-C18)-1 versus 11 J/g for P(Ric-C12)-1. This crystallinity is ascribed to the packing at low temperature of the long alkyl side chains. Surprisingly, the enthalpy of crystallization decreases for the second series, and it even disappears in the case of the high molecular weight PRic-C12. This phenomenon may be interpreted by the lower chain mobility of the polymer chain strongly decreasing the kinetics of crystallization.

As expected, the glass transition temperature (T_g) is also influenced by the nature of the polyester pendant chains. An increase of the T_g with the side chain length is observed. For instance, the T_g of P(Ric-C4)-1 is about –66 °C while the one of P(Ric-C12)-1 is about –61 °C. Moreover, the T_g of P(Ric-Ph) increases due to the phenyl ethyl- pendant chain interactions. As a result, poly(9/10-phenylethylthioether 12-hydroxystearate)s has a T_g between 10 and 15 °C higher than the other

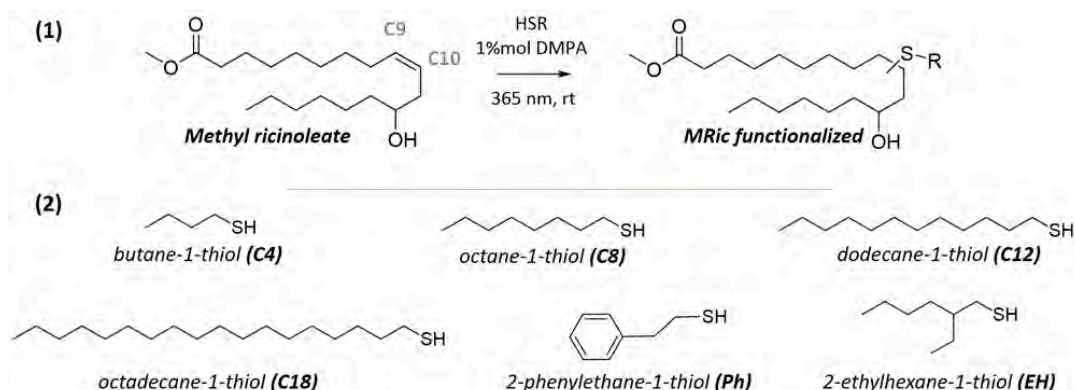


Fig. 3. (1) Methyl ricinoleate functionalization through thiol-ene addition (2) Thiol compounds added as pendant chain on methyl ricinoleate.

Table 2

Methyl ricinoleate functionalization by thiol-ene addition with various thiol compounds.

Monomer	ReactionTime (h)	Ratio RS addition on MRC9: C10 (%) ¹	Yield (%)
MRic-C4	1.5	40: 60	84
MRic-C8	2	35: 65	70
MRic-C12	3	30: 70	67
MRic-C18	3	35: 65	66
MRic-Ph	3	30: 70	70
MRic-EH	4	30: 70	62

¹ Obtained by ¹H NMR.

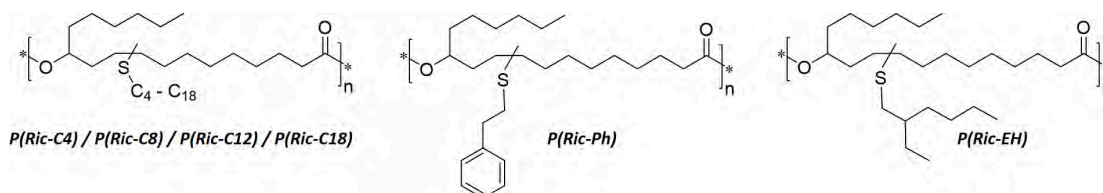
functionalized PRic. The polyester glass transition is also affected by its molar mass, e.g. T_g P(Ric-C4)-1 = -66 °C (M_n = 2600 g·mol⁻¹) and T_g P(Ric-C4)-2 = -62 °C (M_n = 20300 g·mol⁻¹). This is in agreement with Flory-Fox theory [16] due to the decrease of both the general chain mobility and of the influence of chain end by increasing the polymer chain length.

3.4. Investigation of comb poly(9/10-alkylthioether 12-hydroxystearate)s as viscosity modifiers in mineral oil

The comb poly(9/10-alkylthioether 12-hydroxystearate)s were evaluated as viscosity modifiers in mineral oil, Yubase 4 + (as well as in a bio-based oil *i.e.* Radialube 7368 see Table S1). The blends of Yubase 4 + with the polymers were heated at 100 °C for two hours and cooled down to room temperature for one day. As expected, [13] Pric-1 with M_w = 9 000 g·mol⁻¹ was soluble while Pric-2 with M_w = 45

000 g·mol⁻¹ was not. P(Ric-C4) and P(Ric-Ph) were not soluble in Yubase 4 +, whatever their molecular weight, while, branched and long pendant alkyl chains (> 8 carbons) ensure proper polyester solubility in mineral oil whatever the molecular weight. The viscosity of the oil with 3 wt% of soluble comb poly(9/10-alkylthioether 12-hydroxystearate)s added with temperature was evaluated, see Fig. 7. The mass density, dynamic and kinematic values measured between 20 °C and 100 °C are reported in SI (Table S2). The values of relative viscosity, Viscosity Index and Q values are reported in Table 4.

The relative viscosity (η_r) remains stable over the temperature for all the systems evaluated. This stability is even increased by increasing the polyester molecular weight. For instance, Q values for the first series are around 0.9 while reach almost 1 for the second series. Still, no improvement of the oil Viscosity-Temperature behavior (*i.e.* $Q > 1$) was observed. Concerning the thickening efficiency of the comb poly(9-alkyl 12-hydroxystearate)s tested, it appeared for both series than P(Ric-EH) improved more the oil viscosity than other polyesters. For instance, η_r of P(Ric-EH)-2 oil system is about 1.4 while the other relative viscosities are in the range 1.25 – 1.3. P(Ric-EH)-1 increased the Yubase 4 + viscosity to the same range as the commercial additive Viscoplex 10–250 even if its molecular weight is twice lower than the latter. As a result, P(Ric-EH) could be considered as a promising bio-based thickener for mineral base oil. Its thickening efficiency could be attributed to the branched structure of the side chain. Because of its architecture, the side chain may avoid backbone interactions and potential chain coil contraction, leading to a larger coil size in solution. In Fig. 7, the effect of side chain length is not clear as the viscosity appears mostly affected by the polyester molecular weight. For instance, η_r P(Ric-C12)-1 < η_r P(Ric-C18)-1 < η_r P(Ric-C8)-1 for the first series while η_r P(Ric-C8)-2 < η_r P(Ric-C12)-2 < η_r P(Ric-C18)-2 for the second series. In order

**Fig. 4.** Comb polyesters with various pendant chains.**Table 3**

Functionalized methyl ricinoleate conversion (p), degree of polymerization (DP) and comb poly(9-alkyl 12-hydroxystearate) molar mass and thermal properties.

Entry	Time (h)	p^1	DP ¹	M_n^1 (g/mol)	M_n^2 (g/mol)	M_w^2 (g/mol)	\bar{D}^2	$T_{5\%wt}^3$ (°C)	T_g^4 (°C)	T_m^4 (°C)	ΔH_m (J/g)	T_{cris}^4 (°C)	ΔH_c (J/g)
PRic – 1 ^a	8	0.894	9.4	3 000	5 100	9 200	1.8	296	-77	–	–	–	–
P(Ric-C4) – 1 ^a	8	0.947	19	6 400	2 600	6 400	2.4	307	-66	–	–	–	–
P(Ric-C8) – 1 ^a	8	0.944	18	6 000	3 800	8 900	2.3	306	-66	–	–	–	–
P(Ric-C12) – 1 ^a	8	0.925	13	4 500	2 400	5 000	2.1	305	-61	-37 (11 J/g)	-49 (18 J/g)	–	–
P(Ric-C18) – 1 ^a	8	0.934	15	5 200	3 500	7 900	2.3	306	–	-5 (46 J/g)	-12 (50 J/g)	–	–
P(Ric-Ph) – 1 ^a	8	0.910	11	3 800	3 500	9 800	2.8	307	-49	–	–	–	–
P(Ric-EH) – 1 ^a	8	0.945	18	6 300	7 000	21 000	3.1	306	-67	–	–	–	–
PRic – 2 ^b	48	0.977	45	12 400	15 700	45 400	2.9	303	-68	–	–	–	–
P(Ric-C4) – 2 ^b	48	0.972	35	12 100	20 300	44 600	2.2	306	-62	–	–	–	–
P(Ric-C8) – 2 ^b	48	0.989	48	16 600	16 800	34 000	2.1	306	-64	–	–	–	–
P(Ric-C12) – 2 ^b	48	0.962	27	13 000	14 500	36 400	2.5	311	-60	–	–	–	–
P(Ric-C18) – 2 ^b	48	0.988	46	15 800	12 000	44 800	3	312	–	-5 (42 J/g)	-12 (46 J/g)	–	–
P(Ric-Ph) – 2 ^b	48	0.996	72	24 900	23 000	50 000	2.2	306	-44	–	–	–	–
P(Ric-EH) – 2 ^b	48	0.983	60	20 500	20 400	41 300	2	306	-66	–	–	–	–

Reaction conditions: a: Magnetic stirring, 5 wt% of TBD, 140 °C, in the melt under vacuum and b: mechanical stirring 1 wt% of Ti(OiPr)₄ 180 °C, in the melt under vacuum, 200 rpm.

¹ Obtained by ¹H NMR using OCH₃ peak at 3.6 ppm for calculation.² Obtained by SEC in THF –PS calibration.³ Obtained by TGA with a heating ramp of 10 °C. min⁻¹.⁴ Obtained by DSC in the first cooling and second heating at 10 °C.min⁻¹.

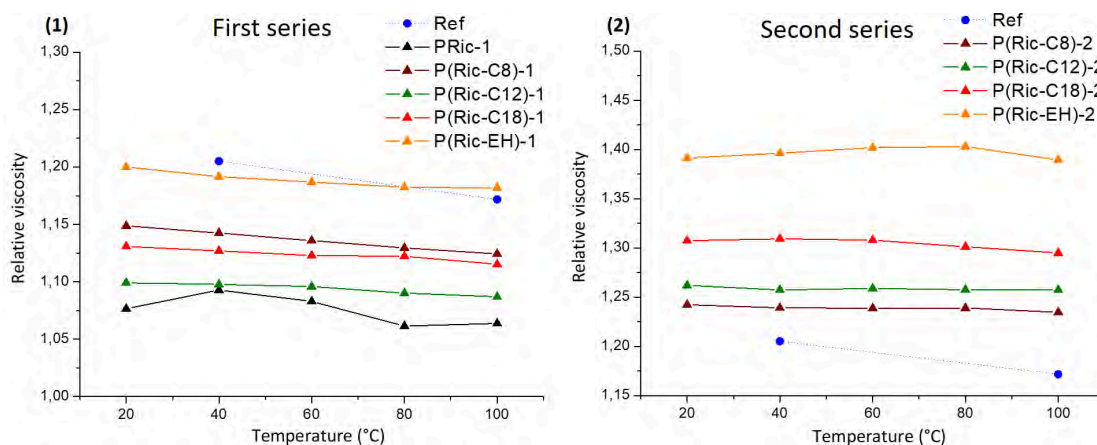


Fig. 7. Relative viscosity (η_r) as a function of temperature for blends of comb polyester at 3 wt% in mineral oil. (1) Comb polyesters with $M_w \approx 10 \text{ kg}\cdot\text{mol}^{-1}$ and (2) with $M_w \approx 45 \text{ kg}\cdot\text{mol}^{-1}$, Reference is Viscoplex 10–250.

Table 4

Relative viscosity (η_r) variation with temperature, Viscosity Index and Q factor of Yubase 4 + and with 3 wt% of comb polyesters with $M_w \approx 10 \text{ kg}\cdot\text{mol}^{-1}$ (first series) and $M_w \approx 45 \text{ kg}\cdot\text{mol}^{-1}$ (second series).

First series $M_w \approx 10 \text{ kg}\cdot\text{mol}^{-1}$								
Mw ($\text{g}\cdot\text{mol}^{-1}$)	Relative viscosity (η_r)					VI	Q	
	20 °C	40 °C	60 °C	80 °C	100 °C			
Viscoplex	40 000	–	1.21	–	–	1.17	163	0.84
PRic – 1	9 200	1.076	1.093	1.083	1.061	1.064	147	0.69
P(Ric-C8) – 1	8 900	1.149	1.143	1.136	1.129	1.124	160	0.87
P(Ric-C12) – 1	5 000	1.099	1.098	1.096	1.090	1.087	156	0.89
P(Ric-C18) – 1	7 900	1.131	1.127	1.123	1.122	1.115	160	0.91
P(Ric-EH) – 1	21 000	1.200	1.192	1.187	1.182	1.182	170	0.95
Second series $M_w \approx 45 \text{ kg}\cdot\text{mol}^{-1}$								
Mw ($\text{g}\cdot\text{mol}^{-1}$)	Relative viscosity (η_r)					VI	Q	
	20 °C	40 °C	60 °C	80 °C	100 °C			
VP	40 000	–	1.205	–	–	1.17	163	0.84
P(Ric-C8) – 2	34 000	1.242	1.239	1.239	1.239	1.235	177	0.98
P(Ric-C12) – 2	36 400	1.262	1.257	1.259	1.258	1.257	181	1.00
P(Ric-C18) – 2	44 800	1.307	1.309	1.308	1.301	1.295	181	0.95
P(Ric-EH) – 2	41 300	1.391	1.396	1.402	1.403	1.390	190	0.98

to highlight the effect of the pendant chain nature on the poly(9-alkyl 12-hydroxystearate)s behavior in solution, the relative viscosity at 100 °C was expressed as a function of the polymer molecular weight in Fig. 8 (1). The Viscosity Index and Q values were reported with respect to the side chain type in Fig. 8 (2).

There is only a weak effect of the nature of the alkyl pendant chain length on the polyester thickening efficiency in mineral oil. P(Ric-C8), P(Ric-C12) and P(Ric-C18) have similar impact on the oil viscosity at 100 °C, whatever their molecular weight. Reversibly, as already shown in Fig. 8, P(Ric-EH) has better thickening efficiency than the other polyesters, leading to a higher VI. It is also visible that non-functionalized PRic has a lower impact on oil viscosity than the polyesters with a second alkyl side chain. This can be explained by a lower solubility of PRic in Yubase 4 + than the other polymers.

To conclude on this part, the comb polyesters synthesized could be used as thickeners both in mineral oils. The side chain nature does not have great influence on the behavior of polyesters in organic oil. Their impact on Viscosity Index seems mainly related to the polymer molecular weight. Some comb poly(9-alkyl 12-hydroxystearate)s such as P(Ric-C4) and P(Ric-Ph) were not soluble in mineral oils. Finally, the poly(9-ethyl hexyl 12-hydroxystearate)s P(Ric-EH) of 21 or 41 $\text{kg}\cdot\text{mol}^{-1}$ showed better thickening efficiency than the other polyesters with a Yubase 4 + with a VI improvement from 145 to 170 or 190 respectively.

3.5 Synthesis of copoly(9-phenylethyl 12-hydroxystearate)-co-(9-dodecane 12-hydroxystearate)

PRics modified by phenyl ethyl moieties (PRic-EH) exhibit very low solubility in the base oil investigated while PRic modified by dodecane shows very high solubility. Thus we decided to produce copolymers of PRic containing these two moieties in order to investigate the VM properties of such copolyester.

Following the polymerization methodology by mechanical stirring, MRic-Ph and MRic-C12 were then copolymerized into copoly(9-phenylethyl 12-hydroxystearate)-co-(9-dodecane 12-hydroxystearate), i.e. P(Ric-Ph-*r*-Ric-C12) with a quantity of phenyl ethyl-moieties ranging from 0 to 40 wt%. Results are summarized in Table 5.

The structures and ratios between the two monomers were confirmed by ^1H NMR spectroscopy; an example is given in Fig. 9 and all the other spectra are reported in Figure S2.

The compositions determined by ^1H NMR analyses are in accordance with the initial monomer feed weight concentrations. The M_n obtained using ^1H NMR and SEC are similar with an average value around 20 000 $\text{g}\cdot\text{mol}^{-1}$ and the M_w value obtained by SEC will be used as reference in the rest of the study (see Figure S3). The obtained bio-based copolyesters were then evaluated as Viscosity Index Improvers in the lubricant based oil Yubase 4 +.

3.6 Evaluation of comb copolyesters as viscosity Index improvers

Firstly, the copolyesters prepared were blended in Yubase 4 + and their solubility in this lubricant was evaluated. The homogeneous blends were then analyzed by viscometry. Mass densities, dynamic and kinematic viscosities were measured from 20 °C to 100 °C, see Table S3. The relative viscosity, the Viscosity Indexes and the Q values are reported in Table 6. The relative viscosities as a function of temperature are displayed on Fig. 10.

The P(Ric-Ph-*r*-Ric-C12)s were insoluble in mineral oil when the weight percentage of phenyl ethyl functionalized monomer was about 30 wt% or above. As a result, only homopolymer P(Ric-C12) and copolyesters with 15 and 25 wt% of MRic-Ph could be evaluated as viscosity modifiers in Yubase 4 +. As illustrated in Fig. 10, the relative viscosity of the two oil solutions containing copolyesters at 3 wt% increase with temperature while the solution with homopolymer remains stable over the whole temperature range. Indeed, the relative viscosity below 60 °C of the oil containing 3 wt% of copolymers 15: 85 and 25: 75, with $M_w = 70 \text{ kg}\cdot\text{mol}^{-1}$ is lower than the one of the oil containing P(Ric-C12) of M_w of 55 $\text{kg}\cdot\text{mol}^{-1}$, while over 60 °C copolymers lead to higher relative viscosities than the homopolymer. The homopolymer addition increases the oil VI from 145 to 181 and the

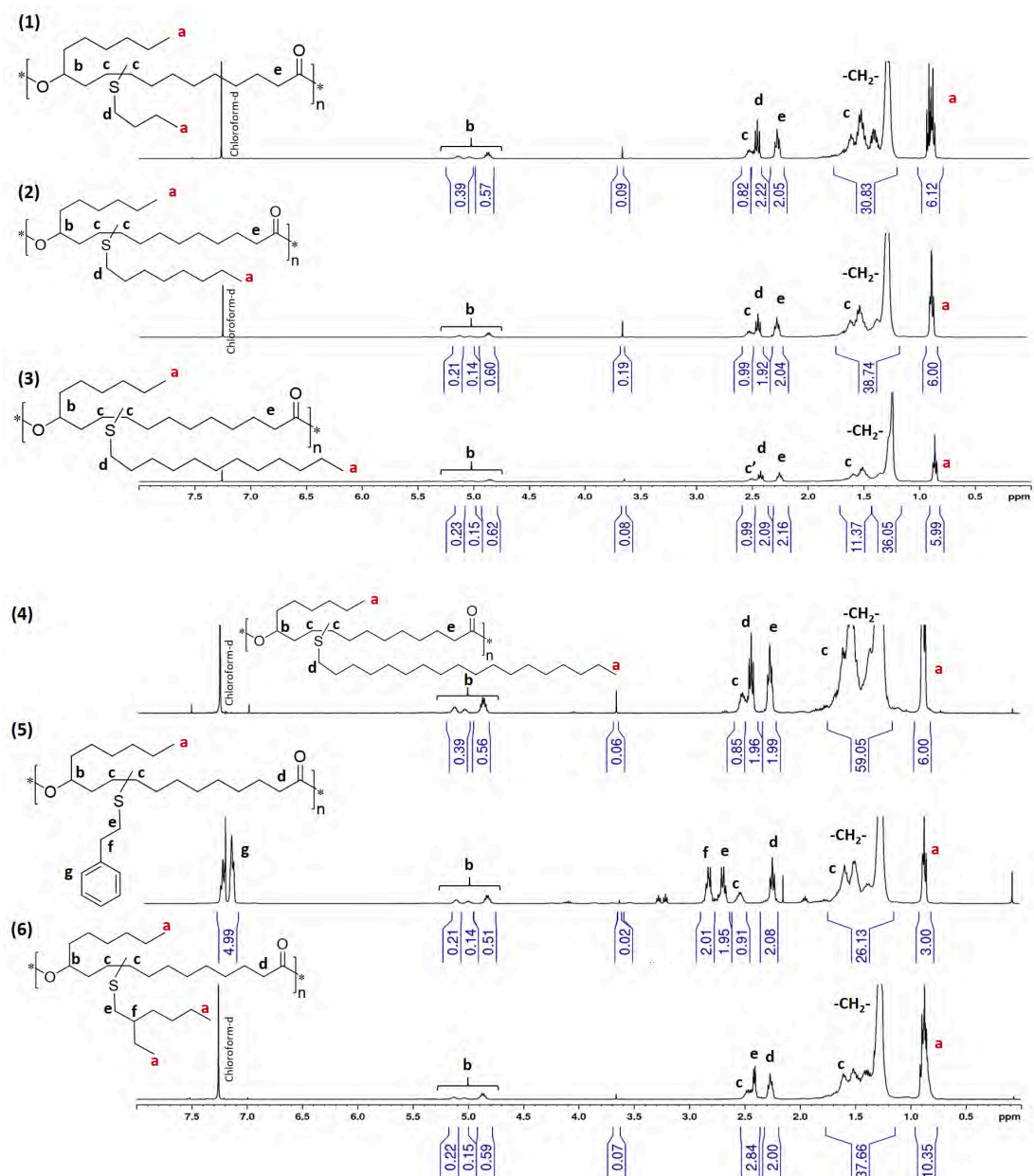


Fig. 5. ¹H NMR spectra of comb polyesters (1) P(Ric-C4) (2) P(Ric-C8) (3) P(Ric-C12) (4) P(Ric-C18) (5) P(Ric-Ph) (6) P(Ric-E).

copolyester addition leads to VI of 186 for 15: 85 and of 189 for 25: 75 copolymers. The Q values of solutions with 15: 85 and 25: 75 copolymers are 1.04 and 1.08 respectively, while with the P(Ric-C12) Q = 0.99. The latter can be then considered as a thickener while the copolyesters are real Viscosity Index improvers with a positive impact on the oil V-T behavior.

It was then speculated that the incorporation of phenyl ethyl group could lead to contracted or aggregated polymer coils at low temperature. It is supposed that the copolyester solubility increases when temperature rises, leading to the relative viscosity increase.

3.7 Study in a model solvent: Conformational behavior

It was assumed that the mineral oil V-T behavior was impacted by some copolyesters such as P(Ric-Ph_{0.25}-r-Ric-C12_{0.75}) due to their low solubility in the oil, the latter increasing when temperature is raised. Conversely, P(Ric-C12), which is more soluble than the copolymer because of the absence of phenyl ethyl pendant group, did not change the

oil viscosity-temperature profile. On the opposite, copolymer addition in oil had an impact on the V-T relationship. It was then anticipated that incorporation of phenyl ethyl moieties in the poly(9-dodecyl 12-hydroxystearate) backbone affects its solubility in Yubase 4 + and its thermal behavior. Collapse or aggregation of polymer coils is observed at room temperature, while chains can expand or disaggregate when temperature is increased, thus leading to the oil VM property. In order to evaluate this phenomena, both the homopolymer P(Ric-C12) and one of the copolymer P(Ric-Ph_{0.25}-r-Ric-C12_{0.75}) were evaluated in *n*-dodecane as a model solvent. At first, the variation of the relative viscosity with temperature was investigated. Then, measurements at different concentration in the dilute regime were performed in order to evaluate the intrinsic viscosity of the polymer in solution $[\eta] = \lim_{c \rightarrow 0} \eta_{sp}/c$ as a function of temperature. Intrinsic viscosity being related to the compacity of the chains, it will give information about the swelling state of the coil.[17] Finally, the polymer coil size variation with temperature was determined by SANS (Small Angle Neutron Scattering)

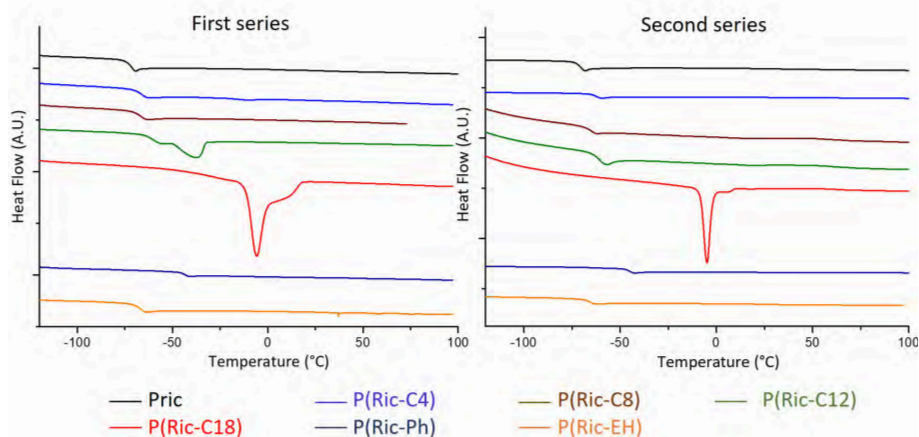


Fig. 6. DSC traces (second heating cycles) of the two series of comb polyesters: first series with $M_w = 10 \text{ kg}\cdot\text{mol}^{-1}$ and second series with $M_w = 45 \text{ kg}\cdot\text{mol}^{-1}$.

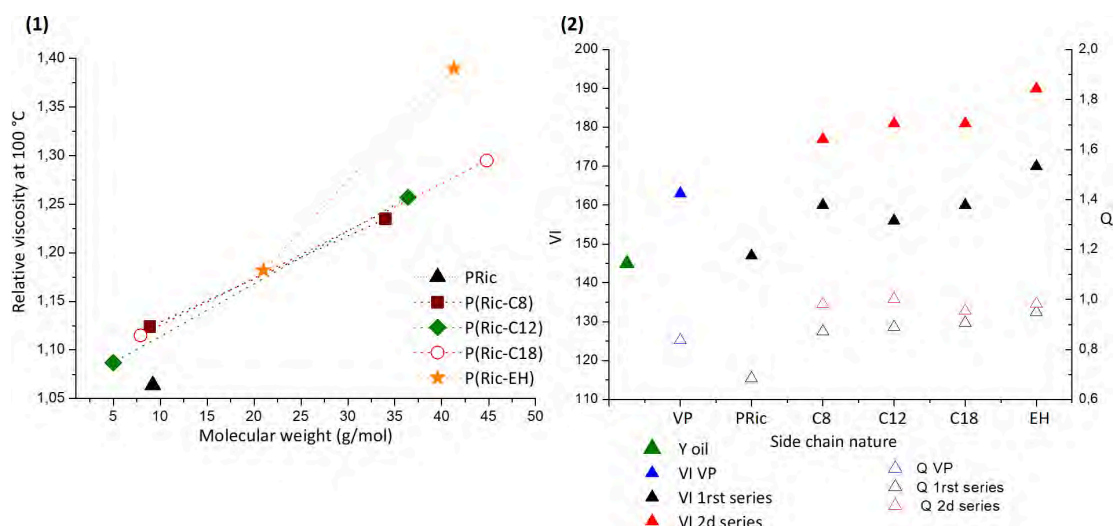


Fig. 8. Yubase 4 + with 3 wt% of comb polyesters (1) Relative viscosity at 100 °C as a function of the polymer M_w . (2) VI and Q values as a function of the nature of the polyester side chains (Y: Yubase 4 + oil, VP: Viscoplex).

Table 5

Ratio of pendant chains (in the feed and after reaction), monomer conversion (p), degree of polymerization (DP) and P(RicPh-*r*-RicC12) values of molecular weights and dispersity deduced by NMR and SEC.

Entry	Feed Ratio (wt.%) Ph: C12	Feed Ratio (mol.%) Ph: C12	Incorporated Ratio (mol.%) ¹ Ph: C12	p^2	DP ²	M_n^2 (g·mol ⁻¹)	M_n^3 (g·mol ⁻¹)	M_w^3 (g·mol ⁻¹)	D^3
P(Ric-C12)	0: 100	0: 100	0: 100	0.983	58	28 000	24 000	55 000	2.2
coP(Ric-Ph/C12)0.85	15: 85	17: 83	19: 81	0.971	35	11 800	22 000	70 500	3.2
coP(Ric-Ph/C12)0.75	25: 75	28: 72	26: 74	0.980	49	16 700	21 500	72 000	3.4
coP(Ric-Ph/C12)0.70	30: 70	33: 67	30: 70	0.976	42	14 400	23 800	85 000	3.6
coP(Ric-Ph/C12)0.65	35: 65	38: 62	34: 66	0.978	45	15 500	19 600	60 600	3.1
coP(Ric-Ph/C12)0.60	40: 60	44: 56	41: 59	0.977	44	15 000	20 000	56 400	2.8

Reaction conditions: 180 °C, 1 wt% of Ti(OiPr)₄ in the melt under vacuum, mechanical stirring, 48 h.

¹ Obtained by ¹H NMR using H_b peak at 2.4 ppm and H_f peak at 2.9 ppm.

² Obtained by ¹H NMR using OCH₃ peak at 3.6 ppm for calculation.

³ Obtained by SEC in THF –calibration PS standards.

measurements, a technique once used to study model polymers for VM applications. More precisely, the apparent molecular weight (M_w) and radius of gyration (R_g) values were measured by SANS. In theory, $Q = [\eta]_{T=100^\circ\text{C}} / [\eta]_{T=40^\circ\text{C}}$ is directly equal to the ratio of molecular volumes in solution $Q = (R_{g|T=100^\circ\text{C}} / R_{g|T=40^\circ\text{C}})$ [3], also called polymer “swelling ratio”.

3.8 Behavior of homo- and copolyester in dodecane with temperature

P(Ric-C12) and P(Ric-Ph_{0.25}-*r*-Ric-C12_{0.75}) were added in dodecane at concentrations varied from 0.3 wt% to 3 wt%. The polymers were solubilized at 100 °C for two hours and cooled down at room temperature without stirring for 24 h. Then, the mass density (ρ), dynamic vis-

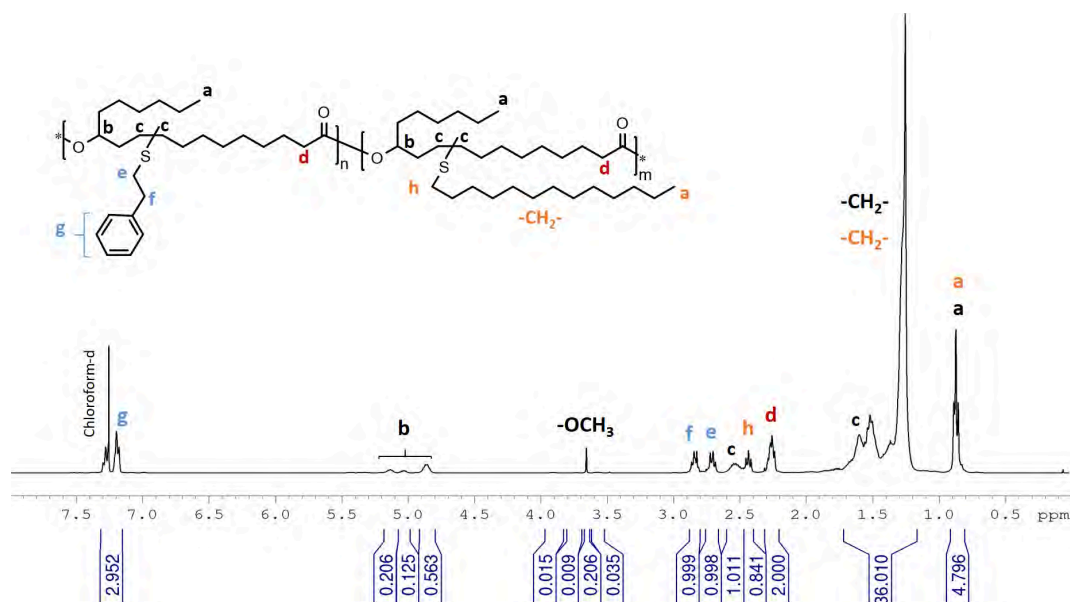


Fig. 9. ^1H NMR spectrum in CDCl_3 of $\text{P}(\text{Ric-Ph}_{0.4}\text{-}r\text{-Ric-C12}_{0.6})$.

Table 6

Solubility, Relative viscosity variation with temperature, Viscosity Index and Q values of Yubase 4 + with 3 wt% of $\text{P}(\text{RicPh-}r\text{-RicC12})$ s with different ratios of phenyl ethyl and dodecyl pendant chains.

Ratio Ph: C12	0: 100	15: 85	25: 75	30: 70	35: 65	40: 60
M_w ($\text{g}\cdot\text{mol}^{-1}$)	55	70	72	85	60	56
	000	500	000	000	600	400
Solubility in Yubase4 + oil	Yes	Yes	Yes	No	No	No
Kinematic viscosity ν ($\text{mm}^2\cdot\text{s}^{-1}$)	40 °C	1.279	1.277	1.276	–	–
	100 °C	1.276	1.288	1.298	–	–
Viscosity Index VI	181	186	189	–	–	–
Q	0.99	1.04	1.08	–	–	–

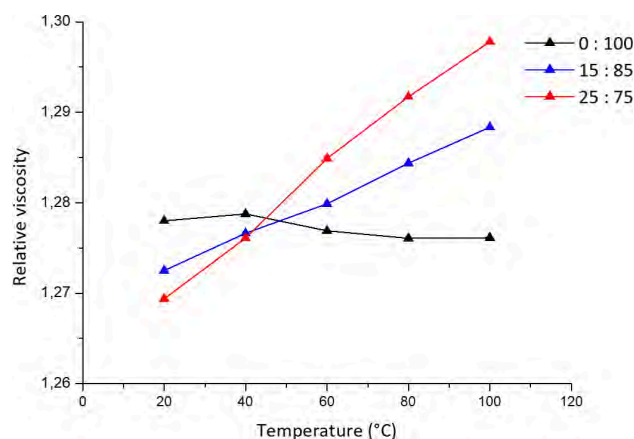


Fig. 10. Relative viscosity as a function of temperature of Yubase 4 + with 3 wt% of second series of comb copolyesters with different ratios of phenyl ethyl and dodecyl pendant chains (Ph: C12).

cosity (η) and kinematic viscosity (ν) of the different solutions at temperature varying from 20 °C to 100 °C were measured using a densitometer-viscosimeter (see Table S4). From these values, the relative viscosity was calculated at each concentration and temperature, as well as the Q values; the latter are reported in Table 7 and can be interpreted – when concentration tends towards 0 – as the chain volume swelling ra-

tios between 40 °C and 100 °C. The relative viscosity variations with respect to temperature are illustrated on Fig. 11.

As expected, the relative viscosity increases with the polymer concentration in dodecane. The Viscosity Index improving effect was higher in the case of the copolymer than for homopolymer, as shown by higher Q values at all concentrations. This feature may be ascribed to the presence of phenyl ethyl pendant chains, as it was observed in the case of polymer addition in mineral oil.

Surprisingly, Q values decrease with concentration for the two polymers, which may be ascribed to contribution of inter-chain attraction (chains preferring to interact together rather than being swollen by the solvent). Both polymers impact positively the *n*-dodecane V-T behavior for concentrations below or equal to 1.3 wt% for P(Ric-C12) and 2.1 wt% for $\text{P}(\text{Ric-Ph}_{0.25}\text{-}r\text{-Ric-C12}_{0.75})$, with $Q > 1$. For higher concentrations, the Q values decrease below one.

This could be due to the regime of dilution. Following literature, the two main phenomena described are the coil expansion and the aggregation/disaggregation behaviors.[9] In dilute solution, polymer coils are hypothetically not in contact with each other. Then, they may be able either to expand or to disaggregate when temperature is raised, leading to an increase of the relative viscosity. Such swelling effect on temperature is clearly visible when plotting the ratio of specific viscosity by concentration $\eta_{sp}/C|_T$ versus C (also called “reduced viscosity”) the intercept of the linear regression being defined as the intrinsic viscosity $[\eta]_T$: for both polymers, the value at 100 °C is higher than at 40 °C, confirming thermal swelling of the chains (see Fig. 11). Conversely, in the semi-dilute regime close to the overlap concentration, C^* , or above, polymer coil interaction or contact may limit either the coil expansion or the disaggregation, leading to lower impact on oil V-T behavior and Q values.

3.9 Determination of the dilute regime

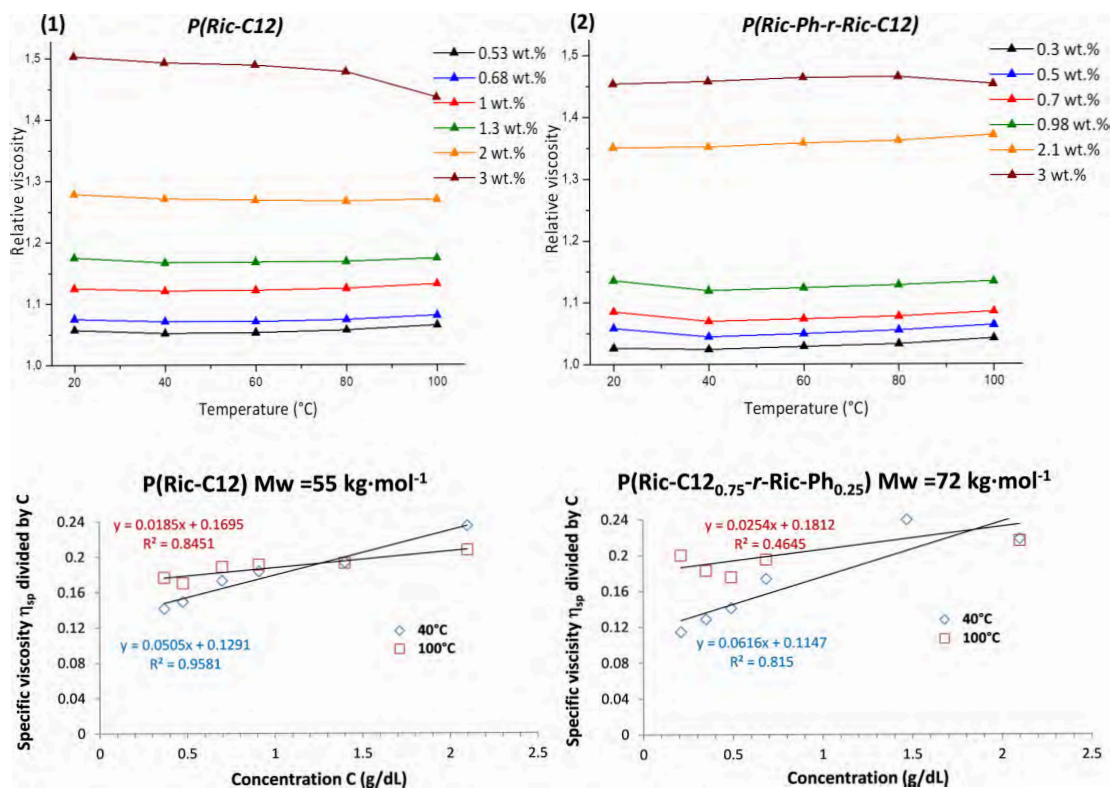
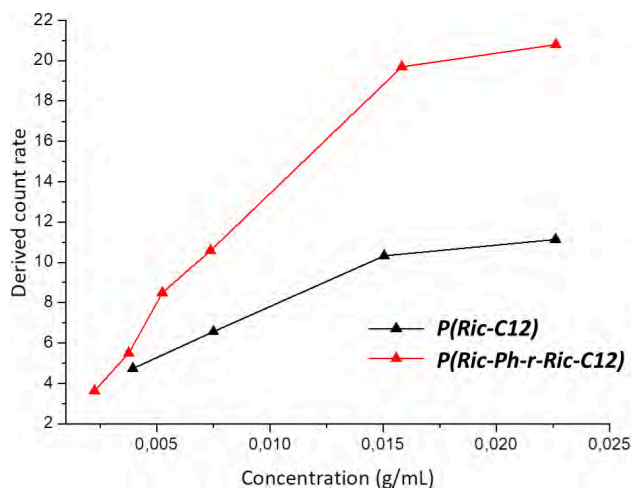
To determine the dilute regime, solutions of dodecane with $\text{P}(\text{Ric-C12})$ and $\text{P}(\text{Ric-Ph}_{0.25}\text{-}r\text{-Ric-C12}_{0.75})$ at concentrations C varied from 2 $\text{mg}\cdot\text{mL}^{-1}$ to 21 $\text{mg}\cdot\text{mL}^{-1}$, i.e. 0.3 wt% – 3 wt%, were analyzed by Dynamic Light Scattering (DLS) at 20 °C and 90° scattering angle. The derived count rates obtained are plotted versus polymer concentration on Fig. 12.

For both polymers in dodecane, the intensity increased linearly with the concentration for $C \leq 0.016 \text{ g}\cdot\text{mL}^{-1}$, i.e. 2 wt%. The polymer coils act as individual particles in solution and the increase of polymer con-

Table 7

Relative viscosity at 40 °C & 100 °C and Q values of P(RicC12 and P(RicPh-r-RicC12) at several concentrations in dodecane.

In dodecane	P(Ric-C12) $M_w = 55 \text{ kg}\cdot\text{mol}^{-1}$						P(Ric-C12 _{0.75} -r-Ric-Ph _{0.25}) $M_w = 72 \text{ kg}\cdot\text{mol}^{-1}$					
Conc. (wt.%)	0.526	0.68	1	1.3	2	3	0.3	0.5	0.7	0.98	2.1	3
η_r 40 °C	1.052	1.071	1.121	1.167	1.271	1.493	1.024	1.045	1.069	1.119	1.352	1.458
100 °C	1.065	1.081	1.132	1.174	1.270	1.436	1.042	1.064	1.086	1.134	1.371	1.454
$Q = \eta_r - 1 _{T=100^\circ\text{C}} / \eta_r - 1 _{T=40^\circ\text{C}}$	1.257	1.149	1.091	1.037	0.994	0.884	1.75	1.426	1.232	1.129	1.056	0.991

**Fig. 11.** Relative viscosity as a function of temperature and reduced viscosity at 40 °C and 100 °C as function of concentration for (1) P(Ric) and (2) P(RicPh-r-RicC12) added in dodecane at various concentrations.**Fig. 12.** Derived count rate as a function of the concentration for homo- and copolyester at 20 °C, performed by DLS measurements at 90 °C scattering angle.

centration in solution leads to a proportional increase of the scattered intensity signal [19] the polyesters are thus in the dilute regime. For concentrations over $0.016 \text{ g}\cdot\text{mL}^{-1}$, the intensity is no more linear, possibly resulting from multiple light scattering, due to polymer chains which start to interact with each other. This concentration is probably close to the overlap concentration C^* . As a result, the polymer cannot be considered anymore in the dilute regime for concentrations above $C = 0.016 \text{ g}\cdot\text{mL}^{-1}$.

In order to confirm this result, the impact of polymer concentration on the solution viscosity was investigated. In dilute regime, the polymer solution viscosity increases linearly with concentration. Then, once C^* is reached, a slope break is observed and the viscosity increase rate as a function of concentration changes; the polymer is then in the “semi-dilute regime” and C^* is called “overlap concentration”. [20] The kinematic viscosity (ν) was evaluated against the concentration of P(Ric-C12) and P(Ric-Ph_{0.25}-r-Ric-C12_{0.75}) in dodecane over the concentration range $0.002 \text{ g}\cdot\text{mL}^{-1} - 0.014 \text{ g}\cdot\text{mL}^{-1}$ and temperature varying from 20 °C to 100 °C. The kinematic viscosities are plotted as a function of polymer concentration on Fig. 13. A linear slope is obtained for the two types of solutions whatever the temperature. The dilute regime is then confirmed over this range of concentrations.

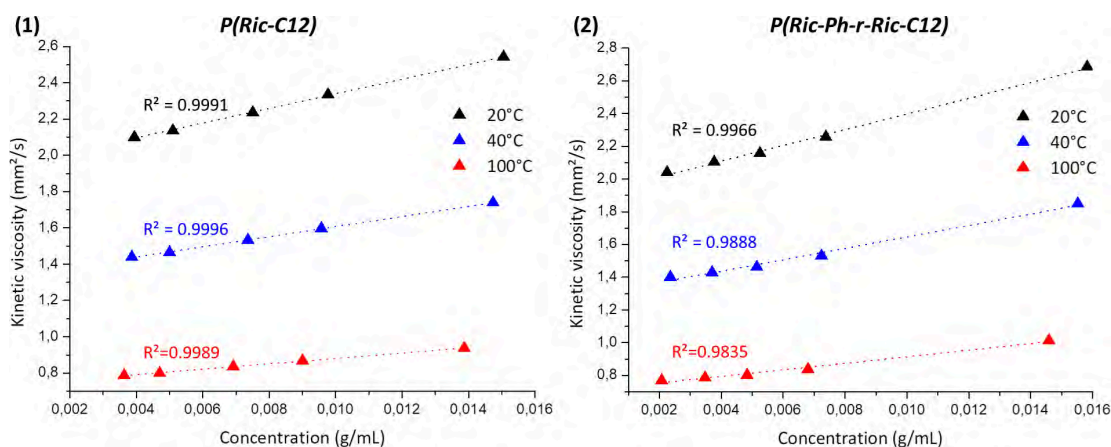


Fig. 13. Kinematic viscosity (v) of dodecane solutions as function of concentration of (1) P(Ric-C12) and (2) P(Ric-Ph-r-RicC12).

3.10 Determination of the intrinsic viscosity

In the dilute regime, the reduced viscosity is calculated according to equation (9).

$$\eta_r = \frac{\eta_{sp}}{c} = \frac{(\eta - \eta_0)/\eta_0}{c} \quad (9)$$

where η_r is called the reduced viscosity, η_{sp} the specific viscosity previously introduced, c the polymer concentration in g·mL⁻¹, η and η_0 are the kinematic viscosities in mm²·s⁻¹ respectively of solution and of pure solvent (*i.e.* dodecane). The reduced viscosity η_r is plotted as a function of the polymer concentration in solution for several temperatures on Fig. 14.

As the polymers are in dilute regime, it is possible to use the Huggins equation (10) to determine the polymer intrinsic viscosity.

$$\eta_r = [\eta] + K_H[\eta]^2 c \quad (10)$$

where $[\eta]$ the intrinsic viscosity in mL·g⁻¹ and K_H the Huggins constant. Using a linear fit of the reduced viscosity as a function of concentration, $[\eta]$ can be obtained at every temperature as the intercept with vertical axis of reduced viscosity for $c \rightarrow 0$. Then the Huggins constants are calculated from the slope values divided by $[\eta]^2$. The values obtained for P(Ric-C12) and P(Ric-Ph_{0.25}-r-Ric-C12_{0.75}) are reported in Table 8.

Generally, the intrinsic viscosity $[\eta]$ of polymers increases with temperature, as ascribed to increased interactions with solvent and chain swelling. In the case of the polyester chains here dissolved in dodecane, the intrinsic viscosity of P(Ric-Ph_{0.25}-r-Ric-C12_{0.75}) is lower than the one of P(Ric-C12) despite the higher molecular weight of the copolymer, *e.g.* at 40 °C, $[\eta] = 8.7$ mL·g⁻¹ with $M_w = 72$ kg·mol⁻¹ and $[\eta] = 12.2$ mL·g⁻¹ with $M_w = 55$ kg·mol⁻¹, respectively. It is then assumed that, due to the presence of phenyl ethyl pendant chains, the copolyester becomes less soluble in dodecane than the poly(9-dodecyl 12-hydroxystearate) homopolymer, thus having a more compact coil conformation, leading to lower intrinsic viscosity.

In the case of P(Ric-C12), the Huggins constant K_H varies from 3 at 40 °C to 0.6 at 100 °C. This variation in the direction opposite to the one of intrinsic viscosity was already observed in literature for Viscosity Index improvers.[13,21] The latter $K_H = 0.6$ is close to 0.5, the mean value generally found for isolated polymers in solution.[22] As a result, P(Ric-C12) chains are presumably aggregated at low temperature and they disaggregate into a solution of individual chains at 100 °C. In parallel to the disaggregation, the polymer affinity with solvent is supposedly enhanced, leading to an increase of the intrinsic viscosity.

A decrease of the K_H values with temperature is also observed for the copolyester, from 12 at 40 °C to 3 at 100 °C. These values are much higher than the ones obtained with P(Ric-C12) solutions, whatever the temperature is. It is then assumed that the P(Ric-Ph-r-Ric-C12) is much

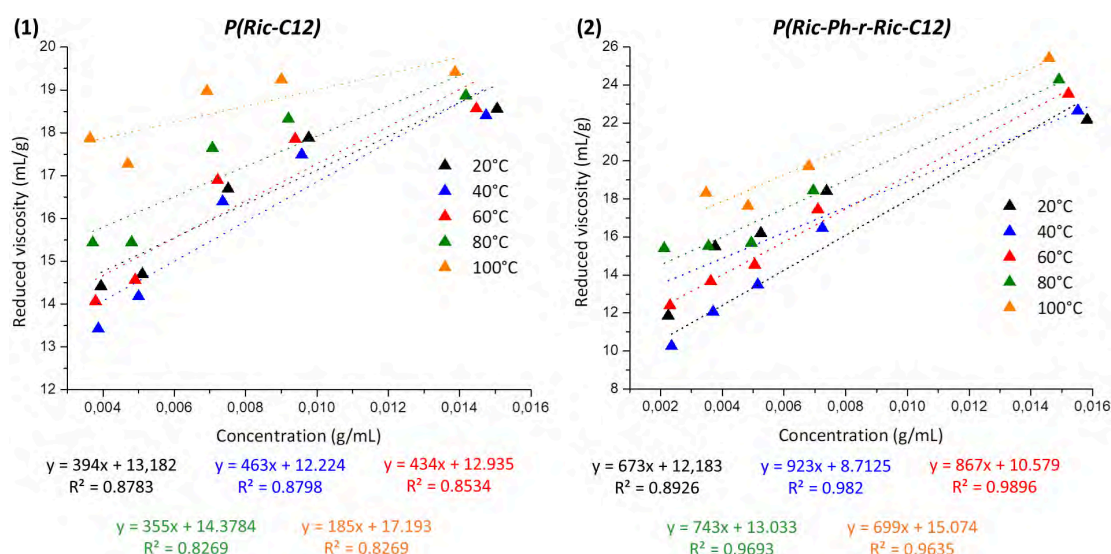


Fig. 14. Reduced viscosity as a function of the (1) P(Ric) and (2) P(Ric-Ph-r-Ric-Ph) concentrations in dodecane at several temperatures.

Table 8

Intrinsic viscosity and Huggins constant at several temperatures of dodecane solutions containing P(Ric-C12) and P(Ric-Ph-r-Ric-C12).

	P(Ric-C12) $M_w = 55 \text{ kg}\cdot\text{mol}^{-1}$		P(Ric-C12-r-Ric-Ph) $M_w = 72 \text{ kg}\cdot\text{mol}^{-1}$	
	$[\eta]$ ($\text{mL}\cdot\text{g}^{-1}$)	K_H	$[\eta]$ ($\text{mL}\cdot\text{g}^{-1}$)	K_H
20 °C	13.18 ± 0.70	2.27 ± 0.49	12.18 ± 1.13	4.53 ± 0.91
40 °C	12.22 ± 0.89	3.10 ± 0.66	8.71 ± 0.59	12.16 ± 0.95
60 °C	12.94 ± 0.91	2.59 ± 0.62	10.58 ± 0.4	7.75 ± 0.45
80 °C	14.38 ± 0.80	1.72 ± 0.45	13.03 ± 0.6	4.38 ± 0.45
100 °C	17.19 ± 0.64	0.62 ± 0.25	15.07 ± 0.82	3.08 ± 0.80

more aggregated in dodecane than P(Ric-C12), leading then to lower $[\eta]$ values. By increasing temperature, the copolymer seems to start to disaggregate. Still, the value $K_H = 3$ at 100 °C indicates that some aggregations may remain and the copolyester chains are not fully dispersed in solution.

3.11 Determination of the polymer size with respect to the temperature

Finally the evolution of the polymer coil size with temperature was also investigated by Small Angle Neutron Scattering (SANS). P(Ric) and P(Ric-Ph- r -Ric-C12 $_{0.75}$) were added in deuterated-dodecane at 0.75 wt% and 3 wt%, *i.e.* below and close to the overlap concentration C^* , respectively. The solutions were stirred at 100 °C for two hours and then cooled down for 24 h. The samples at 0.75 wt% of polymers in dodecane- d_{26} were analyzed following the successive temperatures of 20 °C, 100 °C, 72 °C, 36 °C and then 20 °C for a second time. Two other samples, with polymers at 3 wt% in solution were analyzed at 36 °C and 72 °C. An example of the neutron scattered intensity curve $I(q)$ as a function of the scattering vector are illustrated in Fig. 15. For all the curves, the molar mass M_w and the radius of gyration R_G were obtained using a Debye model fitting, as reported in Table 9.[23–24].

For the two polyesters tested, both the radius of gyration and the effective molar mass slightly decreased when increasing temperature, whatever the concentration was. For instance, when dissolved at

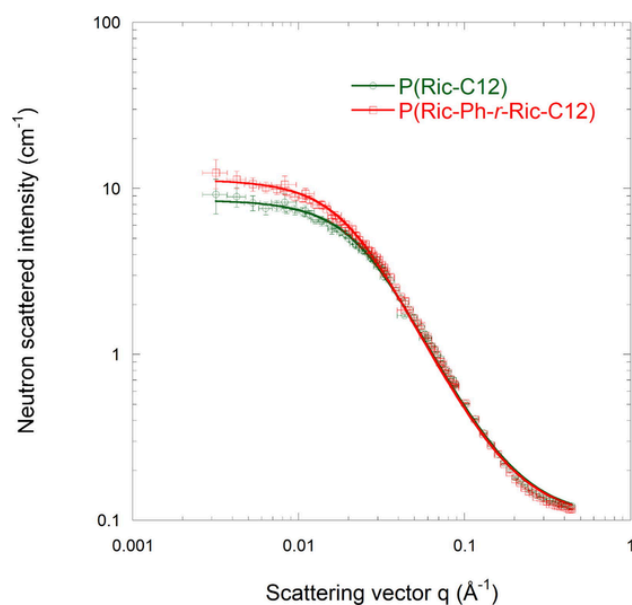


Fig. 15. Neutrons scattered intensity as a function of the modulus of the scattering vector for solutions of dodecane- d_{26} with 3 wt% of P(Ric-C12) and P(Ric-Ph- r -Ric-C12) at 36 °C. The fit parameters are the polymer concentration $c = 0.0226 \text{ g}\cdot\text{cm}^{-3}$, mass density at 36 °C ($0.9382 \text{ g}\cdot\text{cm}^{-3}$) and neutron scattering length density (SLD), respectively $-3.55\cdot 10^8 \text{ cm}^{-2}$ for P(Ric-C12) and $8.80\cdot 10^8 \text{ cm}^{-2}$ for P(Ric-Ph- r -Ric-C12), and SLD of $6.589\cdot 10^{10} \text{ cm}^{-2}$ for dodecane- d_{26} .

Table 9

Radius of gyration R_G and molar mass M_w determined by fitting the SANS data for P(Ric-C12) and P(Ric-Ph-r-Ric-C12) in deuterated dodecane- d_{26} .

In dodecane- d_{26}	M_w ($\text{kg}\cdot\text{mol}^{-1}$) by SEC	Radius of gyration R_G (Å) (Effective M_w in $\text{kg}\cdot\text{mol}^{-1}$)				
		20 °C	100 °C	72 °C	36 °C	20 °C
P(Ric-C12) at 0.75 wt%	55	57.7 (40.7)	57.3 (36.4)	57.2 (36.6)	56.6 (37.2)	54.4 (36.1)
P(Ric-C12) at 3 wt%		–	–	55.7 (29.6)	65.5 (44.7)	–
P(Ric-Ph-r-Ric-C12) at 0.75 wt%	72	65.1 (52.7)	65.4 (45.0)	63.9 (44.2)	63.9 (46.1)	64.6 (51.0)
P(Ric-Ph-r-Ric-C12) at 3 wt%		–	–	67.2 (41.6)	77.2 (61.6)	–

0.75 wt% in dodecane- d_{26} , the P(Ric-C12) has a radius of gyration $R_G = 57.7 \text{ Å}$ and an effective $M_w = 40.7 \text{ kg}\cdot\text{mol}^{-1}$ at 20 °C, which decreased to 57.3 Å and $M_w = 36.4 \text{ kg}\cdot\text{mol}^{-1}$ at 100 °C. These decreases are interpreted by progressive disaggregation of the polymer chains induced by heating, as previously observed in literature.[14] In addition, the R_G and M_w values obtained at 20 °C after the heating cycle remains lower than the ones at the beginning of the experiment, evidencing that the temperature cycle was favorable to better polymer dissolution. Regarding the discrepancy between the molar mass estimated by the Debye fits of the SANS curves and those obtained previously by SEC, one can argue that the latter relied on a calibration with PS standards, therefore the M_w estimates by SANS might be better representative of both polyesters.

It is then speculated that aggregation occurred at 20 °C only after a certain time. The aggregation is slightly enhanced by increasing the polymer concentration. For instance, at 72 °C, P(Ric-Ph- r -Ric-C12) $R_G = 63.9 \text{ Å}$ at 0.75 wt% and $R_G = 67.2 \text{ Å}$ at 3 wt%. The higher the polymer concentration, the higher the aggregation effect, as ascribed to higher inter-chain attractions with polymer concentration.

4. Conclusion

Methyl ricinoleate was functionalized using thiol-ene click chemistry in order to synthesize bio-based comb polyesters with various pendant chains. The obtained poly(9-alkyl 12-hydroxystearate)s were evaluated as Viscosity Index Improvers in a mineral based lubricant. None of the polymers evaluated exhibit VII properties, but at least they can be used as oil thickeners. It appeared that the nature of the pendant side chains affects the polymer solubility in the lubricant base. Copolyesters with a ratio of > 30 wt% of methyl 9-phenyl ethyl 12-hydroxystearate co-monomer were not soluble in mineral oil. However, copolyesters with 15 to 25 wt% of MRic-Ph exhibit a Viscosity Index improver effect, interpreted as due to their limited solubility. In order to confirm this hypothesis and to determine the main mechanisms playing on this phenomenon, a structural study was performed in a model solvent, *n*-dodecane.

Surprisingly, a significant impact of the polymer concentration on their Viscosity Index (VI) improvement efficiency was noticed. It was then hypothesized that the polymer has a positive impact on the oil V-T behavior only in the dilute regime. After determining the concentration range of the latter, the intrinsic viscosity of the two polymers in dodecane was evaluated at various temperatures. For both polymers, the intrinsic viscosity $[\eta]$ increased with temperature, while the Huggins constant decreased. An aggregation-disaggregation behavior was assumed to explain this V-T behavior. The polymer radius of gyration R_G and effective molar mass M_w was then determined for both polymers by SANS measurements. Slight decrease of both R_G and M_w with temperature was observed for both polymers, in agreement with the aggregation –

disaggregation hypothesis. This behavior was even more pronounced for the copolymer bearing phenyl moieties, and thus with lower solubility in dodecane at room temperature. These findings may envision new developments for bio-based polyesters in lubricant applications.

Author Contributions.

The manuscript was written through contributions of all authors. All authors have given approval to the final version of the manuscript. HM performed the experiments, AB and OS performed the SANS analysis.

Declaration of Competing Interest

The authors declare that they have no known competing financial interests or personal relationships that could have appeared to influence the work reported in this paper.

Data availability

Data will be made available on request.

Acknowledgment

This work was performed, in partnership with the SAS PIVERT, within the frame of the French Institute for the Energy Transition (Institut pour la Transition Énergétique (ITE) P.I.V.E.R.T. (www.institut-pivert.com)) selected as an Investment for the Future (“Investissements d’Avenir”). This work was supported, as part of the Investments for the Future, by the French Government under the reference ANR-001-01. The authors thank Equipex Xyloforest ANR-10-EQPX-16. The financial support from the CPER CAMPUSB project funded by the French state and the Région Nouvelle Aquitaine is gratefully acknowledged.

References

- [1] K.C. Ludema, *Friction, wear, lubrication*, CRC Press, 1996.
- [2] D.M. Pirro, M. Webster, E. Daschner, *Lubrication Fundamentals*, Third edition, CRC Press, 2016.
- [3] S. Q. a Rizvi, *A Comprehensive Review of Lubricant Chemistry, Technology, Selection and Design*, ASTM International, 2009.
- [4] R.M. Mortier, M.F. Fox, S.T. Orszulik, *Chemistry and Technology of Lubricants*, Springer, 2010.
- [5] G. Karmakar, K. Dey, P. Ghosh, B.K. Sharma, S.Z. Erhan, *Polymers* 13 (8) (2021) 1333.
- [6] L.R. Rudnick, *Lubricant Additives: Chemistry and Applications*, Taylor and Francis, 2017.
- [7] A. Martini, U.S. Ramasamy, M. Len, *Tribol. Lett.* 66 (2018) 58.
- [8] T.W. Selby, *ASLE Trans.* 1 (1958) 68–81.
- [9] M.J. Covitch, K.J. Trickett, *Adv. Chem. Eng. Sci.* 5 (2015) 134–151.
- [10] P. Cusseau, N. Bouscharain, L. Martinie, D. Philippon, P. Vergne, F. Briand, *Tribol. Trans.* (2017) 1–11.
- [11] C. Williams, F. Brochard, H.L., *Frisch Annu. Rev. Phys. Chem.* 32 (1981) 433–451.
- [12] C. Price, D. Woods, *Polymer (Guildf)*. 15 (1974) 389–392.
- [13] P. Debye, *J. Phys. Colloid Chem.* 51 (1947) 18–32.
- [14] M.T. Savoji, D. Zhao, R.J. Muisener, K. Schimossek, K. Schoeller, T.P. Lodge, M.A. Hillmyer, *Ind. Eng. Chem. Res.* 57 (2018) 1840–1850.
- [15] H. Méheust, J.-F. Le Meins, E. Grau, H. Cramail, *A.C.S. Appl. Polym. Mater.* 3 (2021) 811–818.
- [16] S. Dworakowska, C. Le Coz, G. Chollet, E. Grau, H. Cramail, *Eur. J. Lipid Sci. Technol.* 121 (2019) 1900264.
- [17] ASTM International D2270-10, in *Annual Book of ASTM Standards*, 2015.
- [18] P.J. Flory, T.G. Fox, *J. Am. Chem. Soc.* 73 (5) (1951) 1904–1908.
- [19] H. Benoit, D. Decker, J.S. Higgins, C. Picot, J.-P. Cotton, B. Farnoux, G. Jannink, R. Ober, *Nature Physical Science* 245 (1973) 13–15.
- [20] P.-G. de Gennes, *Scaling Concepts in Polymer Physics*, 1979, Cornell University Press.
- [21] T.G. Fox, P. J. Flory *J. App. Phys.* 2 (1950) 581–591.
- [22] E. Maderek, B.A. Wolf, *Angew. Makromol, Chemie* 161 (1988) 157–173.
- [23] A.S. Yeung, C.W. Frank, *Polymer* 31 (1990) 2089–2100.
- [24] *Polymers and neutron scattering by J. Higgins and H. Benoit, Clarendon Press, Oxford, UK, 1994. p.160.*

Supporting information

Fatty-acid based comb copolyesters as Viscosity Index Improvers in Lubricants

Hélène Méheust,¹ Jean-François Le Meins,¹ Annie Brûlet,² Olivier Sandre,¹ Etienne Grau,¹

Henri Cramail^{1}*

Henri.Cramail@enscbp.fr

Number of pages: 6

Number of Figures: 3

Number of Tables: 4

Table S1: Radialube 7368 with 3 wt.% of comb polyesters. Density, dynamic (η) and kinematic (ν) viscosities values at several temperatures

First series $M_w \approx 10 \text{ kg.mol}^{-1}$						
	Temperature	20°C	40°C	60°C	80°C	100°C
Radialube 7368	Density	0.94	0.93	0.91	0.90	0.88
	η (mPa.s)	42.91	19.05	9.96	5.96	4.13
	ν (mm ² .s ⁻¹)	45.56	20.55	10.91	6.64	4.67
+3%wt Priolube	Density	0.9419	0.9275	0.9133	0.899	0.8865
	η (mPa.s)	58.41	25.22	13.04	7.75	5.30
	ν (mm ² .s ⁻¹)	62.01	27.19	14.28	8.625	5.98
+3%wt PRic-1	Density	0.9417	0.9273	0.913	0.8987	0.8848
	η (mPa.s)	48.34	21.08	10.99	6.57	4.53
	ν (mm ² .s ⁻¹)	51.34	22.73	12.03	7.31	5.12
+3%wt P(Ric-C4)-1	Density	0.9424	0.928	0.9138	0.8995	0.8854
	η (mPa.s)	52.43	22.58	11.64	6.93	4.75
	ν (mm ² .s ⁻¹)	55.63	24.33	12.74	7.70	5.36
+3%wt P(Ric-C8)-1	Density	0.9426	0.928	0.9139	0.9	0.8856
	η (mPa.s)	51.7	22.3	11.55	6.88	4.73
	ν (mm ² .s ⁻¹)	54.85	24.03	12.64	7.65	5.34
+3%wt P(Ric-C12)-1	Density	0.9415	0.9271	0.9128	0.8986	0.8845
	η (mPa.s)	49.81	21.5	11.13	6.64	4.56
	ν (mm ² .s ⁻¹)	52.9	23.19	12.2	7.385	5.20
+3%wt P(Ric-C18)-1	Density	0.9412	0.9267	0.9124	0.8982	0.884
	η (mPa.s)	49.44	21.46	11.16	6.67	4.59
	ν (mm ² .s ⁻¹)	52.54	23.16	12.23	7.41	5.19
+3%wt P(Ric-Ph)-1	Density	0.9438	0.9294	0.9151	0.9009	0.8871
	η (mPa.s)	53.92	23.2	11.94	7.09	4.86
	ν (mm ² .s ⁻¹)	57.14	24.97	13.04	7.87	5.47
+3%wt P(Ric-EH)-1	Density	0.9421	0.9277	0.9134	0.8992	0.885
	η (mPa.s)	57.58	24.76	12.69	7.51	5.11
	ν (mm ² .s ⁻¹)	61.13	26.68	13.9	8.35	5.77
Second series $M_w \approx 45 \text{ kg.mol}^{-1}$						
	Temperature	20°C	40°C	60°C	80°C	100°C
+3%wt PRic-2	Density	0.9416	0.9276	0.9133	0.8991	0.8848
	η (mPa.s)	58.82	25.31	12.98	7.68	5.26
	ν (mm ² .s ⁻¹)	62.45	27.29	14.21	8.54	5.94
+3%wt P(Ric-C4)-2	Density	0.9424	0.928	0.9137	0.8995	0.8854
	η (mPa.s)	65.24	27.84	14.29	8.46	5.76
	ν (mm ² .s ⁻¹)	69.23	30	15.64	9.41	6.51
+3%wt P(Ric-C8)-2	Density	0.9419	0.9276	0.9133	0.8991	0.8849
	η (mPa.s)	60.37	25.98	13.42	7.99	5.46
	ν (mm ² .s ⁻¹)	64.09	28.01	14.69	8.88	6.17
+3%wt P(Ric-C12)-2	Density	0.9416	0.9272	0.913	0.8988	0.8846
	η (mPa.s)	60.22	26	13.39	7.97	5.46
	ν (mm ² .s ⁻¹)	63.95	28.05	14.66	8.86	6.17
+3%wt P(Ric-C18)-2	Density	0.9411	0.9268	0.9125	0.8983	0.8844
	η (mPa.s)	60.39	26.11	13.51	8.05	5.51
	ν (mm ² .s ⁻¹)	64.17	28.17	14.81	8.97	6.23

+3%wt P(Ric-Ph)-2	Density	0.9438	0.9295	0.9152	0.901	0.8868
	η (mPa.s)	65.52	27.88	14.29	9.45	5.76
	ν (mm²·s⁻¹)	69.42	30	15.62	9.383	6.502
+3%wt P(Ric-EH)-2	Density	0.9421	0.9277	0.9134	0.8992	0.8850
	η (mPa.s)	65.87	28.09	14.42	8.54	5.80
	ν (mm²·s⁻¹)	69.92	30.28	15.78	9.50	6.56

Table S2: Yubase 4+ with 3 wt.% of comb polyesters. Density, dynamic (η) and kinematic (ν) viscosities values at several temperatures

First series $M_w \approx 10 \text{ kg.mol}^{-1}$						
	Temperature	20°C	40°C	60°C	80°C	100°C
Yubase 4+	Density	0.8226	0.8099	0.7973	0.7846	0.7720
	η (mPa.s)	34.41	15.16	7.97	4.82	3.35
	ν (mm²·s⁻¹)	41.82	18.71	9.99	6.14	4.34
+3%wt VP	Density	-	-	-	-	-
	η (mPa.s)	-	-	-	-	-
	ν (mm²·s⁻¹)	-	22.552	-	-	5.082
+3%wt PRic-1	Density	0.8254	0.8127	0.8	0.7874	0.7748
	η (mPa.s)	37.16	16.62	8.656	5.13	3.57
	ν (mm²·s⁻¹)	45.02	20.45	10.82	6.51	4.61
+3%wt P(Ric-C8)-1	Density	0.8257	0.813	0.8003	0.7877	0.7751
	η (mPa.s)	39.67	17.39	9.086	5.46	3.78
	ν (mm²·s⁻¹)	48.04	21.38	11.35	6.93	4.87
+3%wt P(Ric-C12)-1	Density	0.8255	0.8128	0.8001	0.7874	0.7748
	η (mPa.s)	37.94	16.69	8.76	5.27	3.65
	ν (mm²·s⁻¹)	45.96	20.54	10.95	6.69	4.71
+3%wt P(Ric-C18)-1	Density	0.8252	0.8125	0.7998	0.7872	0.7745
	η (mPa.s)	39.02	17.14	8.977	5.42	3.75
	ν (mm²·s⁻¹)	47.29	21.09	11.22	6.89	4.84
+3%wt P(Ric-EH)-1	Density	0.8257	0.8131	0.8004	0.7878	0.7751
	η (mPa.s)	41.44	18.13	9.492	5.72	3.97
	ν (mm²·s⁻¹)	50.19	22.3	11.86	7.26	5.12
Second series $M_w \approx 45 \text{ kg.mol}^{-1}$						
	Temperature	20°C	40°C	60°C	80°C	100°C
+3%wt P(Ric-C8)-2	Density	0.8257	0.813	0.8004	0.7877	0.7751
	η (mPa.s)	42.9	18.86	9.907	5.99	4.151
	ν (mm²·s⁻¹)	51.96	23.19	12.38	7.60	5.35
+3%wt P(Ric-C12)-2	Density	0.8255	0.8128	0.8002	0.7876	0.7749
	η (mPa.s)	43.57	19.63	10.06	6.08	4.23
	ν (mm²·s⁻¹)	52.78	23.53	12.58	7.72	5.45
+3%wt P(Ric-C18)-2	Density	0.825	0.8125	0.7998	0.7872	0.7752
	η (mPa.s)	45.12	19.9	10.45	6.29	4.35
	ν (mm²·s⁻¹)	54.68	24.5	13.07	7.99	5.62
+3%wt P(Ric-EH)-2	Density	0.8259	0.8132	0.8006	0.7879	0.7753
	η (mPa.s)	48.06	21.25	11.22	6.79	4.67
	ν (mm²·s⁻¹)	58.19	26.13	14.01	8.61	6.03

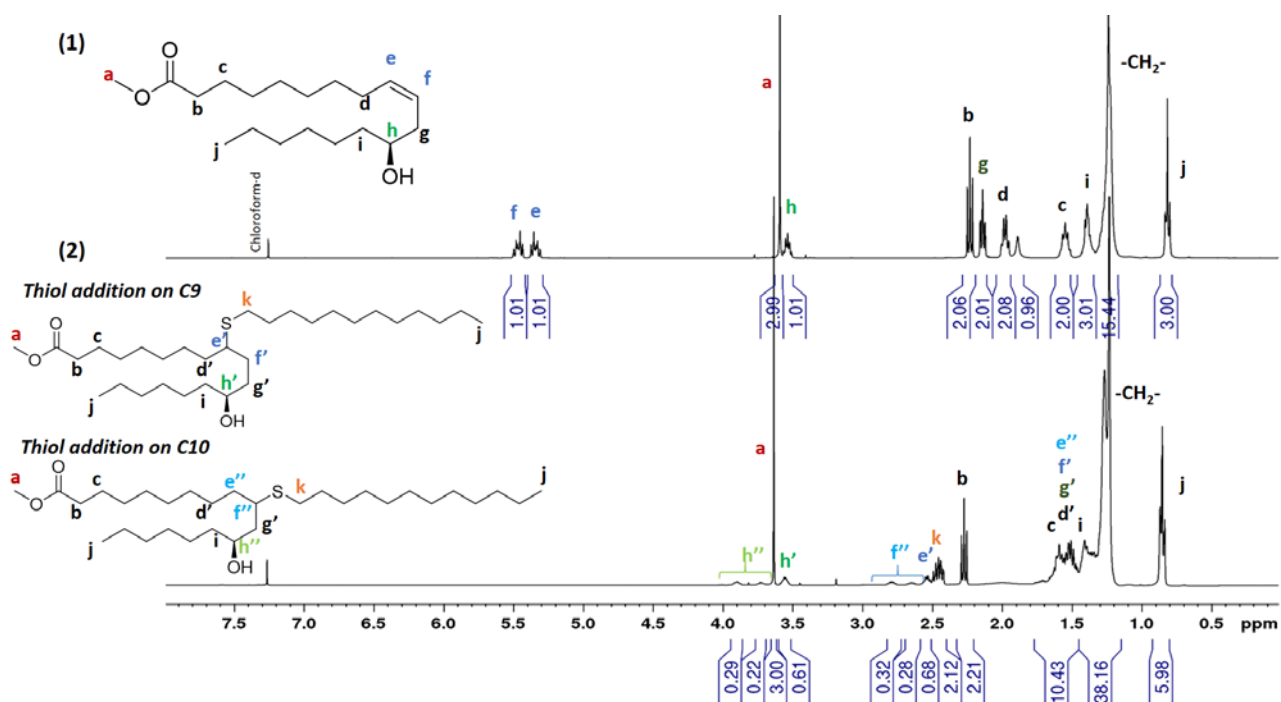


Figure S1: ^1H NMR spectra in CDCl_3 of (1) methyl ricinoleate and (2) methyl 9-alkyl 12-hydroxystearate

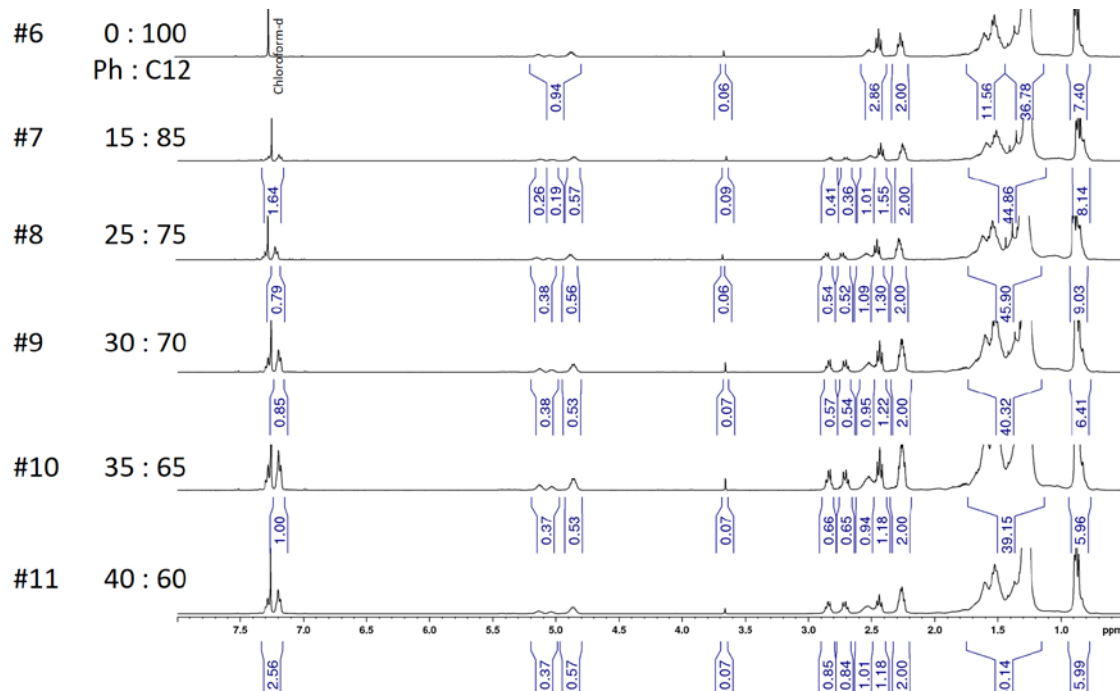


Figure S2: ^1H NMR spectra in CDCl_3 of $\text{P}(\text{Ric-Ph-}r\text{-Ric-C12})$ with phenyl and dodecane pendant chains at different ratios of each. $M_w = 60 \text{ kg}\cdot\text{mol}^{-1}$

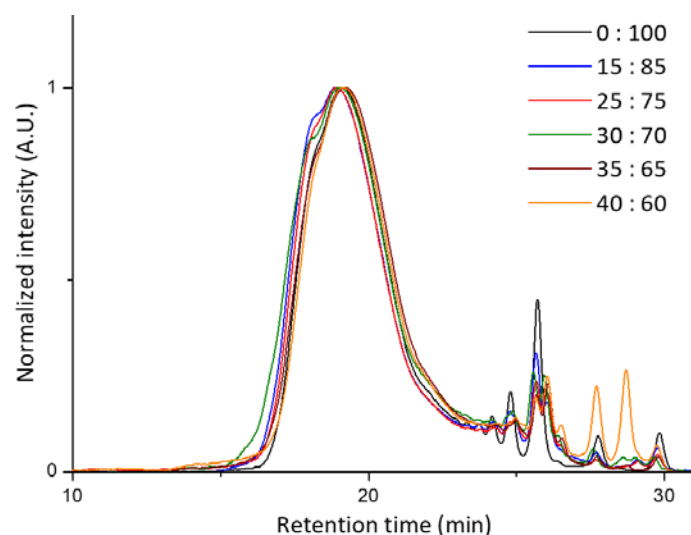


Figure S3 SEC traces of P(RicPh-r-RicC12) s with different ratio of phenyl ethyl and dodecyl pendant chains

Table S3: Yubase 4+ with 3 wt.% copolyesters with $M_w = 50 \text{ kg.mol}^{-1}$. Density, dynamic (η) and kinematic (ν) viscosities values at several temperatures

	Temperature	20°C	40°C	60°C	80°C	100°C
Yubase 4+	Density	0.8226	0.8099	0.7973	0.7846	0.7720
	η (mPa.s)	34.41	15.16	7.97	4.82	3.35
	ν (mm ² ·s ⁻¹)	41.82	18.71	9.99	6.14	4.34
Y+3 wt.% Viscoplex	Density	-	-	-	-	-
	η (mPa.s)	-	-	-	-	-
	ν (mm ² ·s ⁻¹)	-	22.552	-	-	5.082
#6 Y+3 wt.% P(Ric-C12)	Density	0.8255	0.8128	0.8001	0.7875	0.7748
	η (mPa.s)	44.12	19.45	10.21	6.17	4.29
	ν (mm ² ·s ⁻¹)	53.45	23.93	12.76	7.83	5.54
#7 Y+3 wt% P(Ric-Ph-r-Ric-C12) Ratio 15 : 85	Density	0.8259	0.8132	0.8005	0.7879	0.7753
	η (mPa.s)	43.96	19.43	10.24	6.21	4.33
	ν (mm ² ·s ⁻¹)	53.22	23.89	12.79	7.88	5.59
#8 Y+3 wt% P(Ric-Ph-r-Ric-C12) Ratio 25 : 75	Density	0.826	0.8133	0.8007	0.788	0.7754
	η (mPa.s)	43.86	19.42	10.28	6.25	4.36
	ν (mm ² ·s ⁻¹)	53.09	23.88	12.84	7.93	5.63

Table S4: Dodecane with P(Ric-C12) or P(Ric-Ph-r-Ric-C12) at several concentrations. Density, dynamic (η) and kinematic (ν) viscosities values at several temperatures

	Temperature	20°C	40°C	60°C	80°C	100°C
Dodecane 99%	Density	0.7494	0.7349	0.7202	0.7054	0.6903
	η (mPa.s)	1.459	1.005	0.757	0.628	0.51
	ν (mm².s⁻¹)	1.987	1.368	1.050	0.890	0.739
D + 0.53 wt.% P(Ric-C12)	Density	0.75	0.7355	0.7208	0.706	0.691
	η (mPa.s)	1.575	1.058	0.797	0.665	0.544
	ν (mm².s⁻¹)	2.100	1.439	1.106	0.941	0.787
D + 0.68 wt.% P(Ric-C12)	Density	0.7503	0.7357	0.7211	0.7063	0.6912
	η (mPa.s)	1.602	1.078	0.811	0.675	0.552
	ν (mm².s⁻¹)	2.136	1.465	1.125	0.956	0.799
D + 1 wt.% P(Ric-C12)	Density	0.7508	0.7363	0.7217	0.7069	0.6918
	η (mPa.s)	1.679	1.129	0.85	0.708	0.578
	ν (mm².s⁻¹)	2.236	1.533	1.178	1.001	0.836
D + 1.3 wt.% P(Ric-C12)	Density	0.7514	0.7369	0.7223	0.7075	0.6924
	η (mPa.s)	1.754	1.177	0.885	0.735	0.600
	ν (mm².s⁻¹)	2.334	1.597	1.226	1.040	0.867
D + 2 wt.% P(Ric-C12)	Density	0.7525	0.738	0.7234	0.7086	0.6936
	η (mPa.s)	1.913	1.283	0.964	0.799	0.651
	ν (mm².s⁻¹)	2.542	1.739	1.332	1.128	0.938
D + 3 wt.% P(Ric-C12)	Density	0.7538	0.7394	0.7247	0.71	0.695
	η (mPa.s)	2.252	1.511	1.133	0.934	0.737
	ν (mm².s⁻¹)	2.987	2.043	1.563	1.315	1.061
D + 0.3 wt% P(Ric-Ph-r-Ric-C12) Ratio 25 : 75	Density	0.7496	0.735	0.7204	0.7055	0.6904
	η (mPa.s)	1.529	1.030	0.778	0.649	0.532
	ν (mm².s⁻¹)	2.040	1.401	1.080	0.919	0.770
D + 0.5 wt% P(Ric-Ph-r-Ric-C12) Ratio 25 : 75	Density	0.7497	0.7351	0.7204	0.7056	0.6906
	η (mPa.s)	1.577	1.050	0.793	0.662	0.542
	ν (mm².s⁻¹)	2.103	1.429	1.102	0.939	0.786
D + 0.7 wt% P(Ric-Ph-r-Ric-C12) Ratio 25 : 75	Density	0.7501	0.7356	0.7209	0.7061	0.691
	η (mPa.s)	1.617	1.076	0.812	0.677	0.554
	ν (mm².s⁻¹)	2.156	1.463	1.127	0.959	0.802
D + 0.98 wt% P(Ric-Ph-r-Ric-C12) Ratio 25 : 75	Density	0.7508	0.7363	0.7217	0.7068	0.692
	η (mPa.s)	1.694	1.128	0.851	0.710	0.580
	ν (mm².s⁻¹)	2.257	1.531	1.180	1.004	0.838
D + 2.1 wt% P(Ric-Ph-r-Ric-C12) Ratio 25 : 75	Density	0.7536	0.7392	0.7246	0.7099	0.6948
	η (mPa.s)	2.023	1.367	1.033	0.860	0.704
	ν (mm².s⁻¹)	2.684	1.849	1.426	1.212	1.013
D + 3 wt% P(Ric-Ph-r-Ric-C12) Ratio 25 : 75	Density	0.754	0.7395	0.7249	0.7101	0.6951
	η (mPa.s)	2.178	1.475	1.114	0.926	0.747
	ν (mm².s⁻¹)	2.889	1.994	1.537	1.304	1.074